

Recent results and future plans of the COMPASS Collaboration

The COMPASS Experiment at CERN SPS

Spectroscopy and π polarizabilities

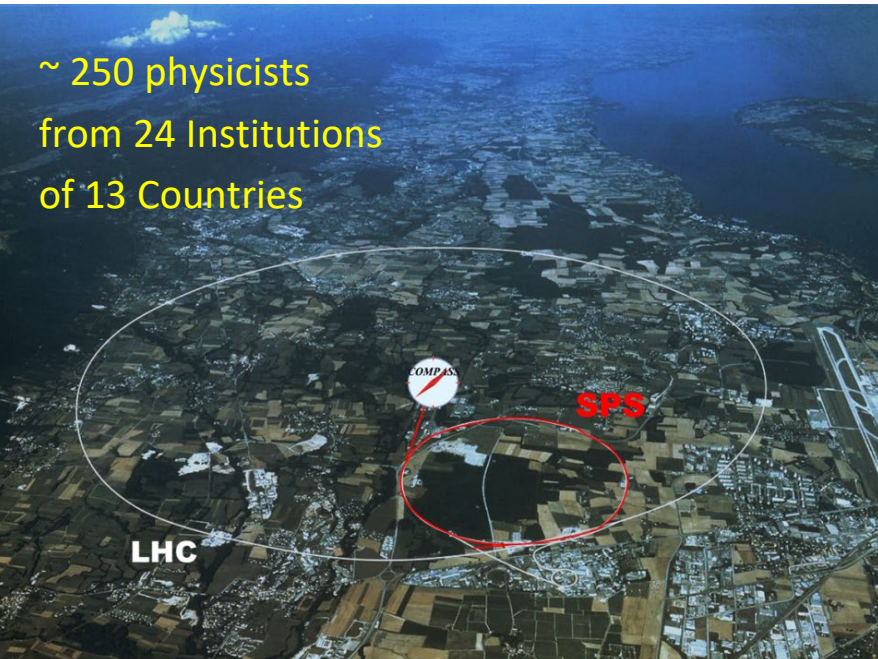
The hadron structure

2021-22: Tensor charge and proton radius

M2 beam line: Lol for a QCD Facility at CERN

14-18 settembre 2020

*Stefano Levorato
on behalf of the COMPASS collaboration*



Experiments with muon beam:

COMPASS - I (2002 – 2011)

- Spin structure, Gluon polarization
- Flavor decomposition
- Transversity
- Transverse Momentum-dependent PDF

COMPASS - II (2012 – 2021) ...

- DVCS and HEMP
- Unpolarized SIDIS and TMDs

	Дубна (LPP and LNP), Москва (INR, LPI, State University), Протвино
	Warsawa (NCBJ), Warsawa (TU) Warsawa (U)
	Praha (CU/CTU) Liberec (TU) Brno (ISI-ASCR)
	Calcutta (Matriviani)
	Taipei (AS)
	CERN
	Yamagata
	Lisboa/Aveiro
	Tel Aviv
	Bochum, Bonn (ISKP & PI), Erlangen, Freiburg, Mainz, München TU
	USA (UIUC)
	Saclay
	Torino (University, INFN), Trieste (University, INFN)

Experiments with hadron beams:

- Pion polarizability
- Diffractive and Central production
- Light meson spectroscopy
- Baryon spectroscopy

- Pion and Kaon polarizabilities
- Drell-Yan studies

Proposed physics programme:

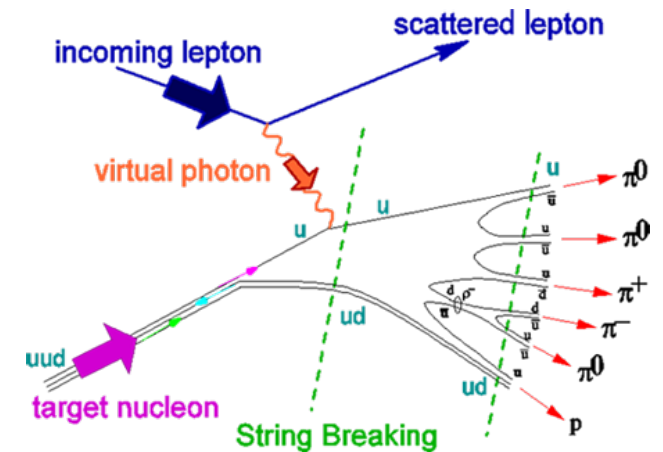
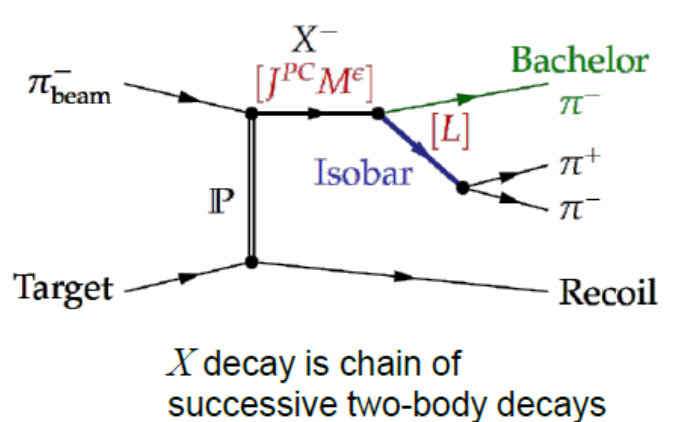
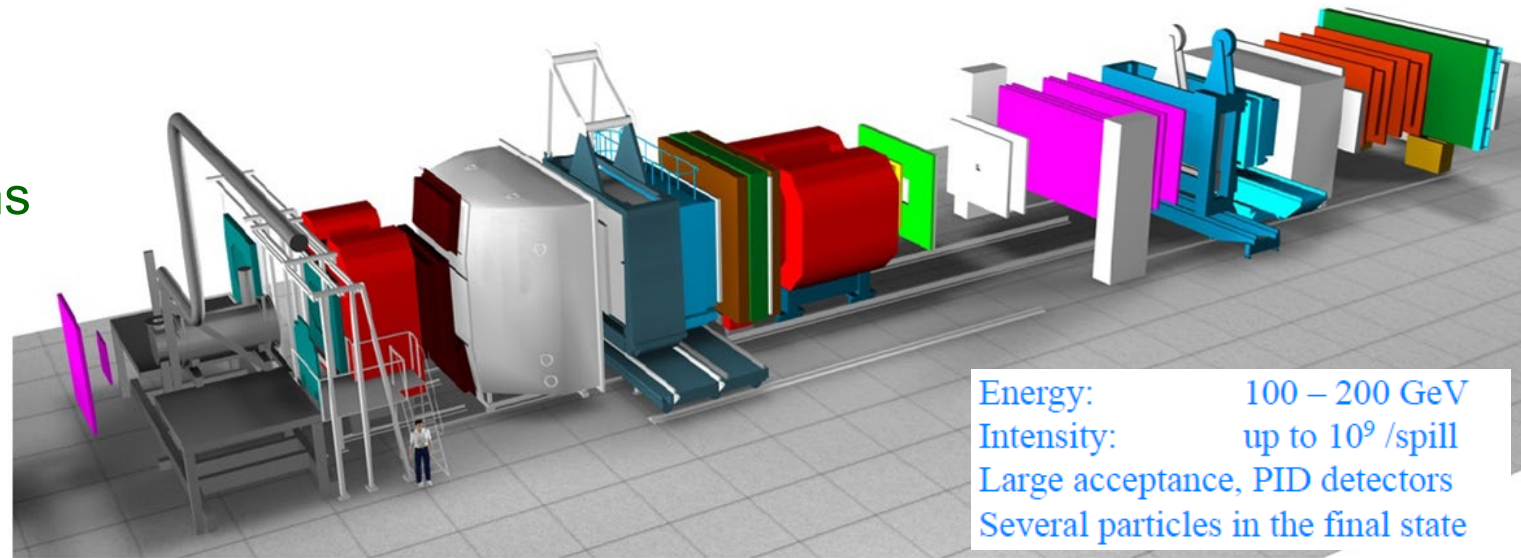
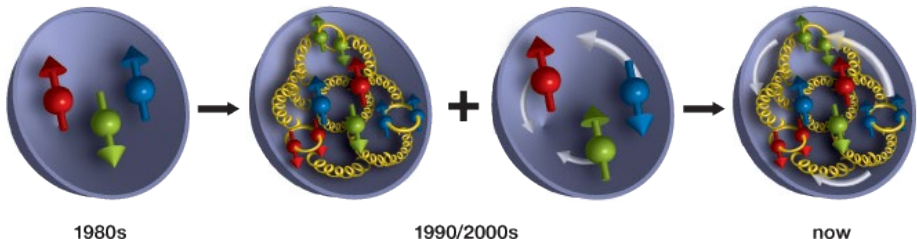
hadron spectroscopy (p, π, K)

- light mesons, glue-balls, exotic mesons
- polarisability of pion and kaon

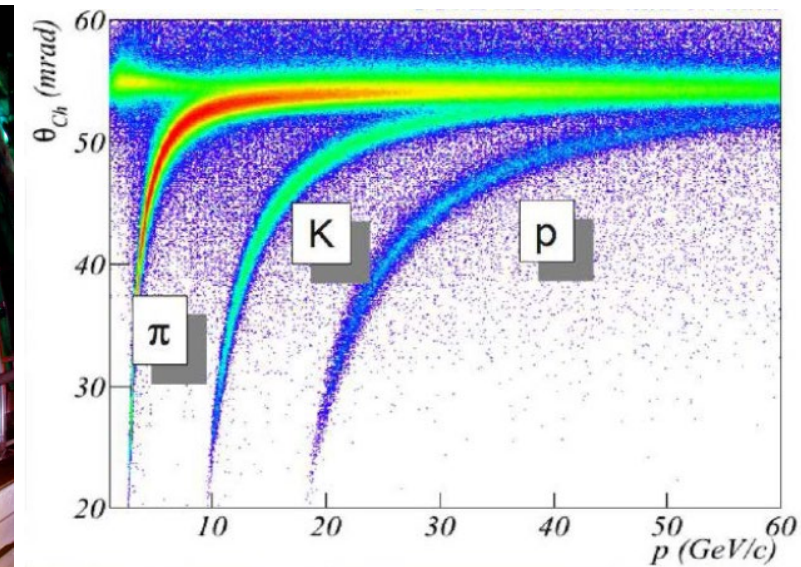
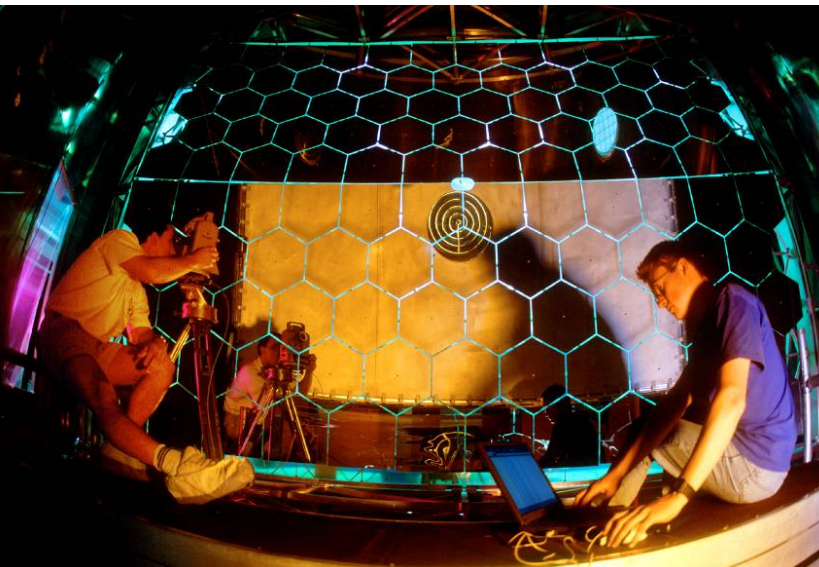
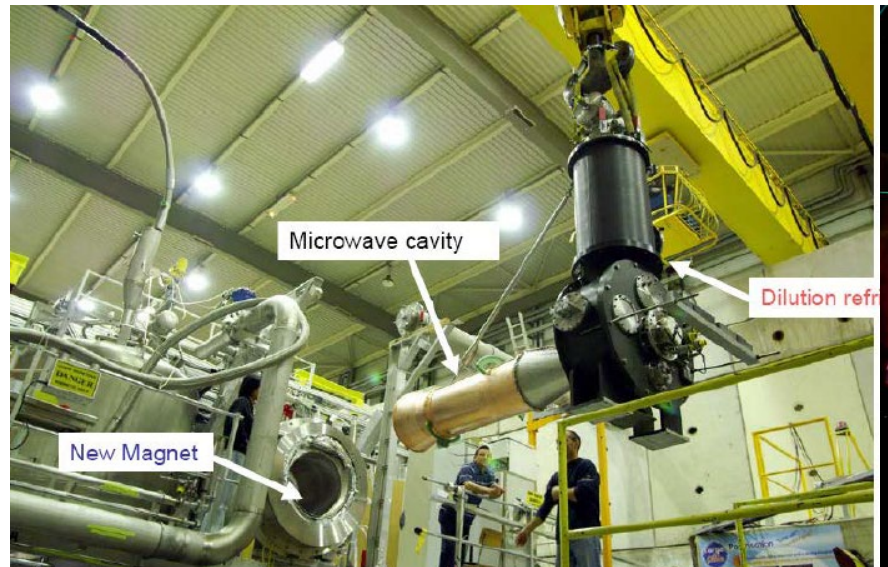
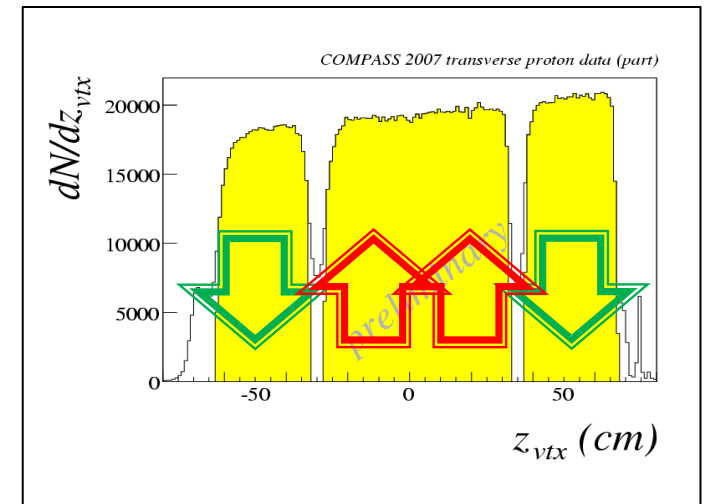
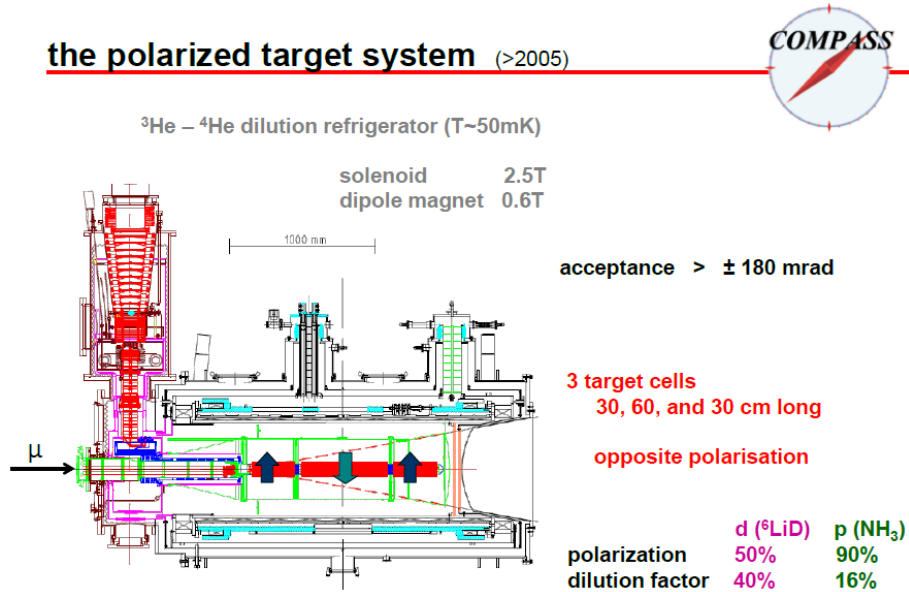
nucleon structure (μ)

- longitudinal spin structure - SIDIS
- transverse spin structure - SIDIS

- Drell-Yan (π)
- DVCS (SIDIS) (μ)

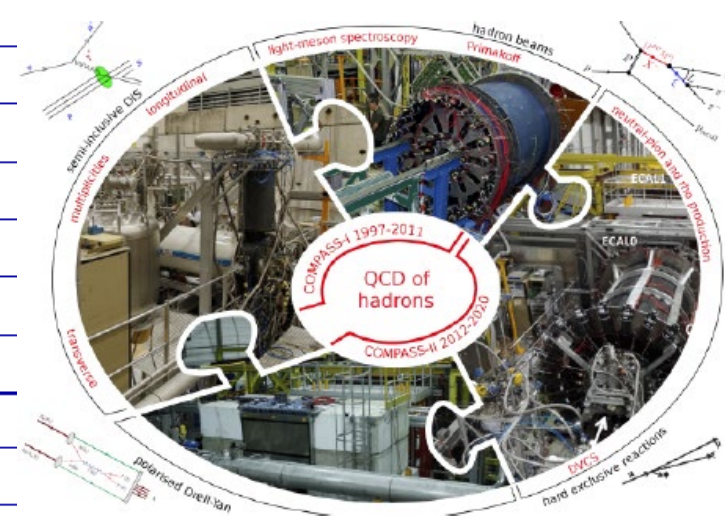


the polarized target system (>2005)



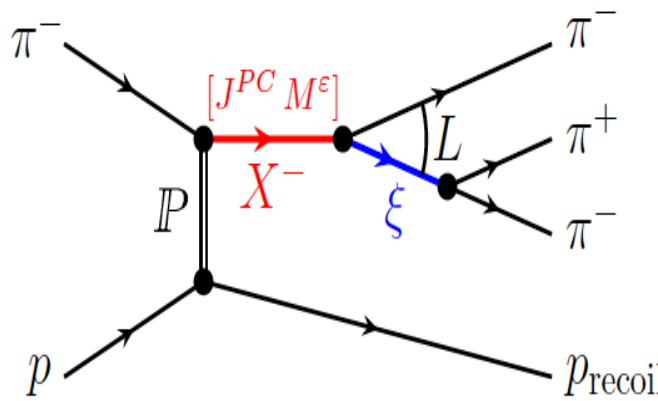
Wide physics programme

2002	nucleon structure with	160 GeV μ	L&T	polarised deuteron target
2003	nucleon structure with	160 GeV μ	L&T	polarised deuteron target
2004	nucleon structure with	160 GeV μ	L&T	polarised deuteron target
2005	CERN accelerators shut down			
2006	nucleon structure with	160 GeV μ	L	polarised deuteron target
2007	nucleon structure with	160 GeV μ	L&T	polarised proton target
2008	hadron spectroscopy			
2009	hadron spectroscopy			
2010	nucleon structure with	160 GeV μ	T	polarised proton target
2011	nucleon structure with	190 GeV μ	L	polarised proton target
2012	Primakoff & DVCS / SIDIS test			
2013	CERN accelerators shut down			
2014	Test beam Drell-Yan process with π beam and T polarised proton target			
2015	Drell-Yan process with π beam and T polarised proton target			
2016	DVCS / SIDIS with μ beam and unpolarised proton target			
2017	DVCS / SIDIS with μ beam and unpolarised proton target			
2018	Drell-Yan process with π beam and T polarised proton target			
2021	nucleon structure with 160 GeV μ	T polarized deuteron target		



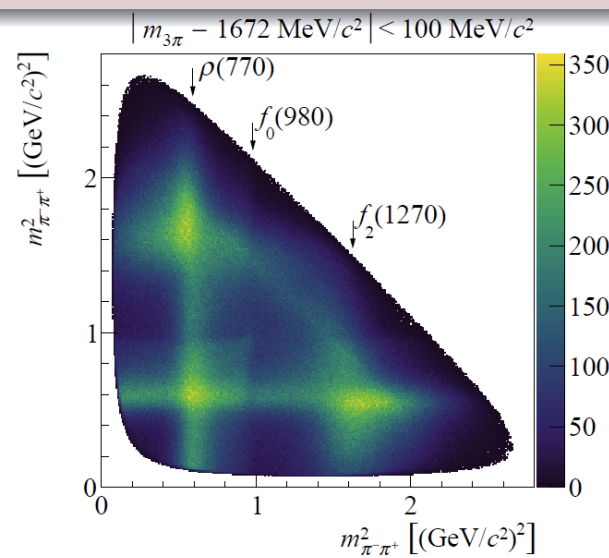
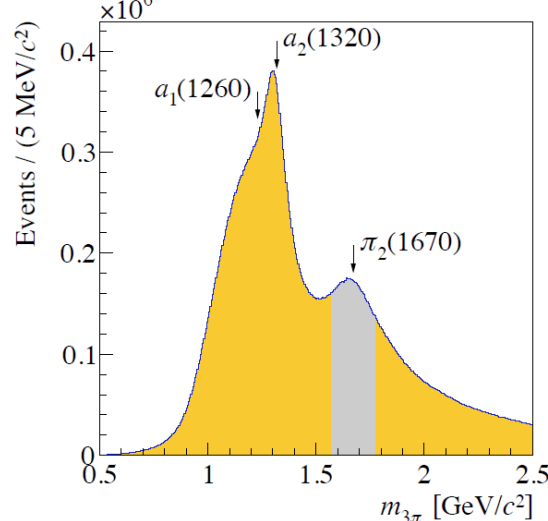
2008-2009 data taking, 190 GeV/c hadron beam on a hydrogen target.

COMPASS has performed the most comprehensive analysis of isovector resonances decaying into $\eta\pi$, $\eta'\pi$, or $\pi^-\pi^-\pi^+$ final states.



Isobar Model: X decay is a chain of successive two body decays

- $46 \times 10^6 \pi^-\pi^-\pi^+$ events \Rightarrow approx. 10 \times previous experiments

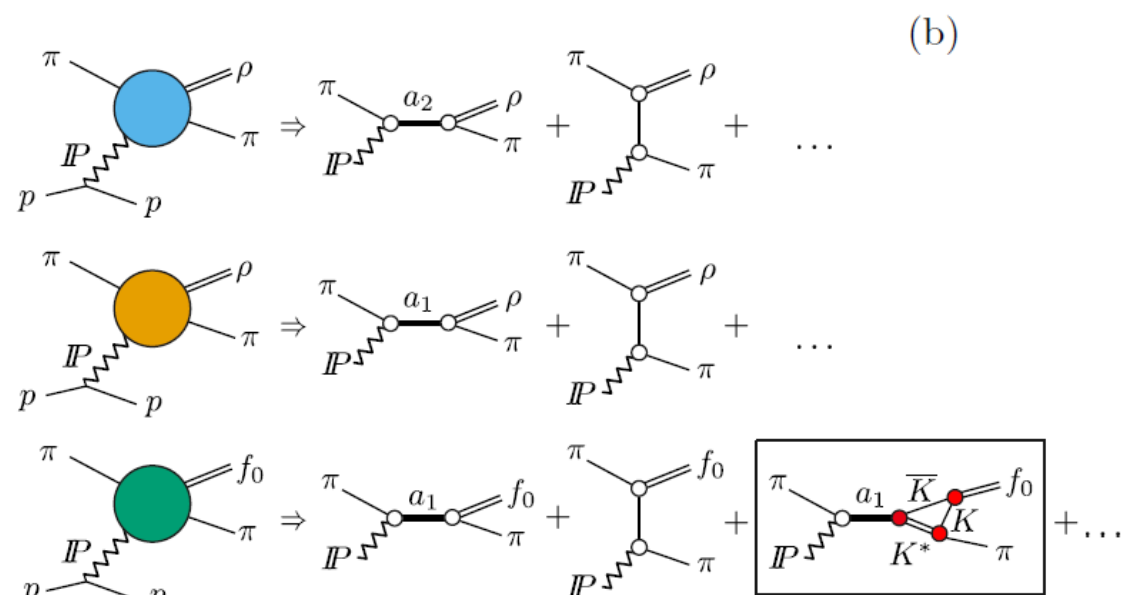
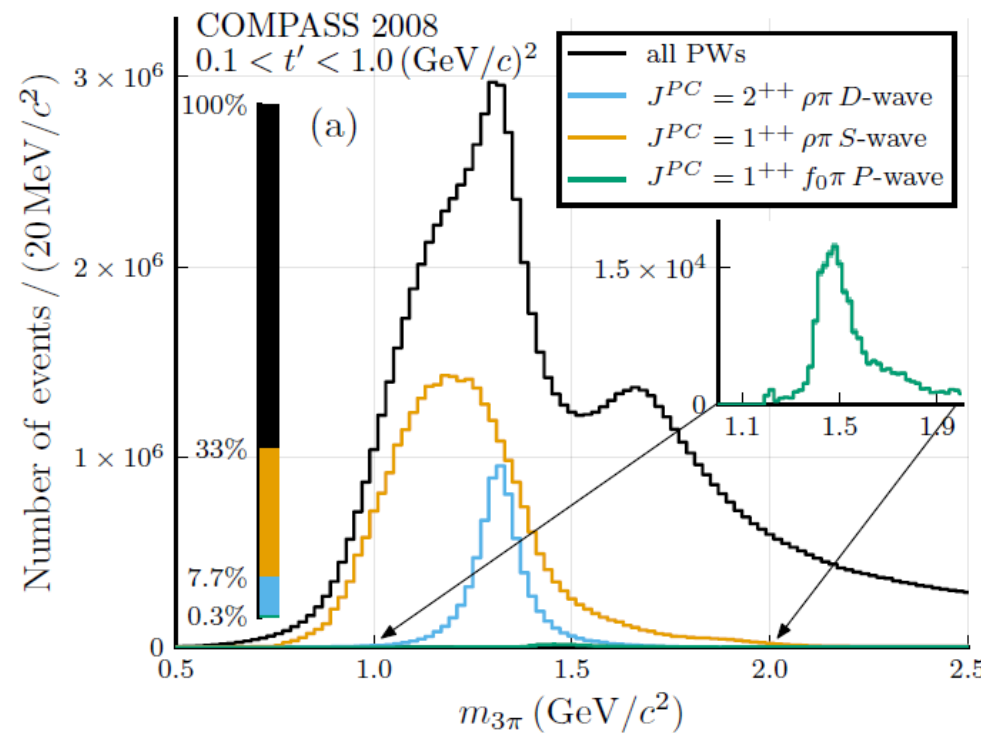


"Light-meson spectroscopy with COMPASS", Progress in Particle and Nuclear Physics 11 (July 2020) 103755

- Partial Wave analysis (PWA) in mass bins up to 88 waves
- Fit of spin density matrix for major waves with Breit-Wigner

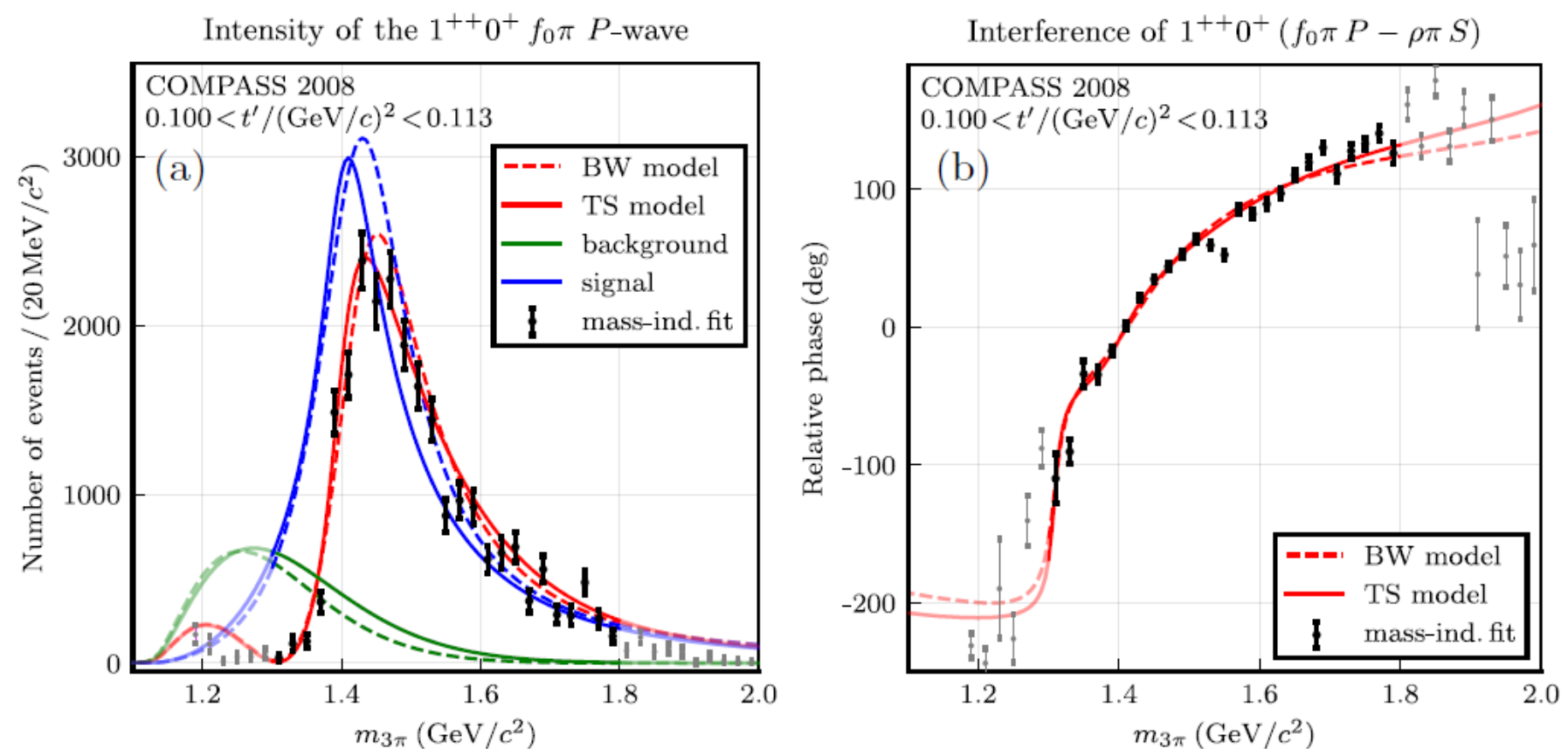
Collaboration with Joint Physics Analysis Center (JPAC)

Resonance-like signal, $a_1(1420)$, found in the $f_0(980) \pi^- P\ 1++$ partial wave, [PRL 115, 082001 \(2015\)](#) not fitting into the $q\bar{q}$ scheme of ordinary mesons Interpretations: tetraquark, molecule-like, etc.

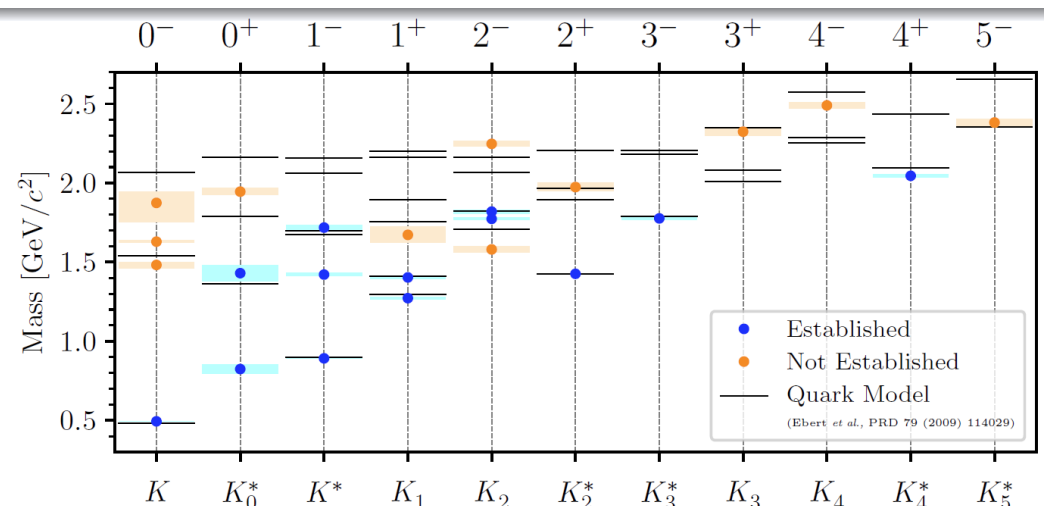


Kinematic effect (triangle singularity) in the decay of $a_1(1260)$ into $K^*(892) \bar{K} + \text{c.c.}$, and rescattering of the \bar{K} with the K from the K^* decay into the observed $f_0(980)$

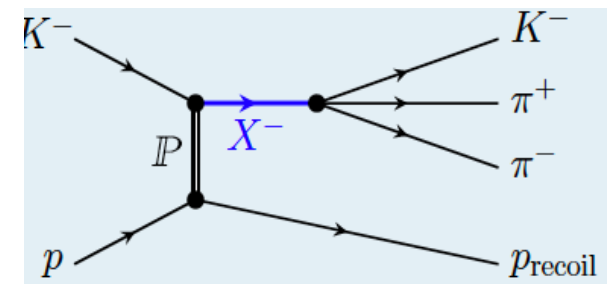
The Triangle Singularity (TS) model is fitted to our partial-wave data.
Less parameters than the resonance hypothesis (BW). TS fit has slightly better quality → no need for an additional resonance.



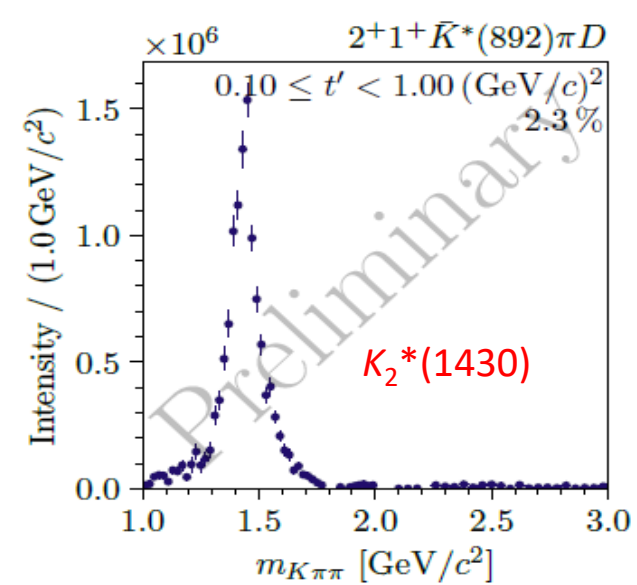
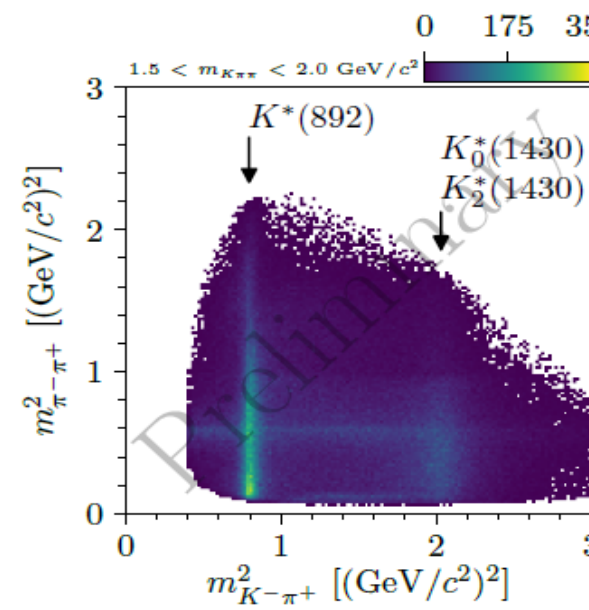
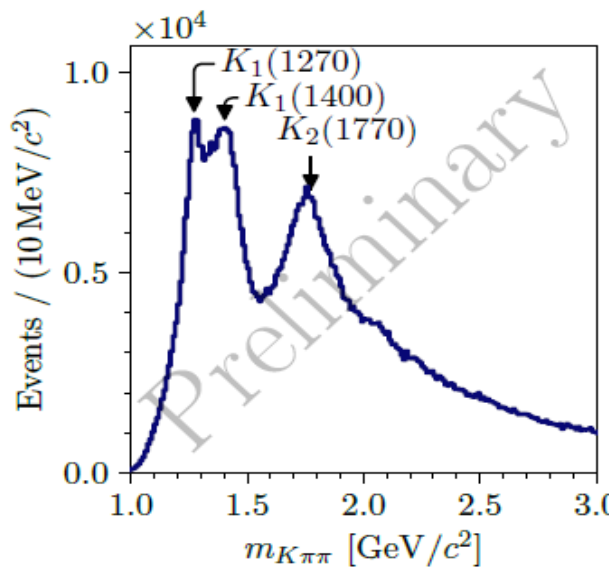
The PDG lists 25 kaon states, 12 of which need confirmation.



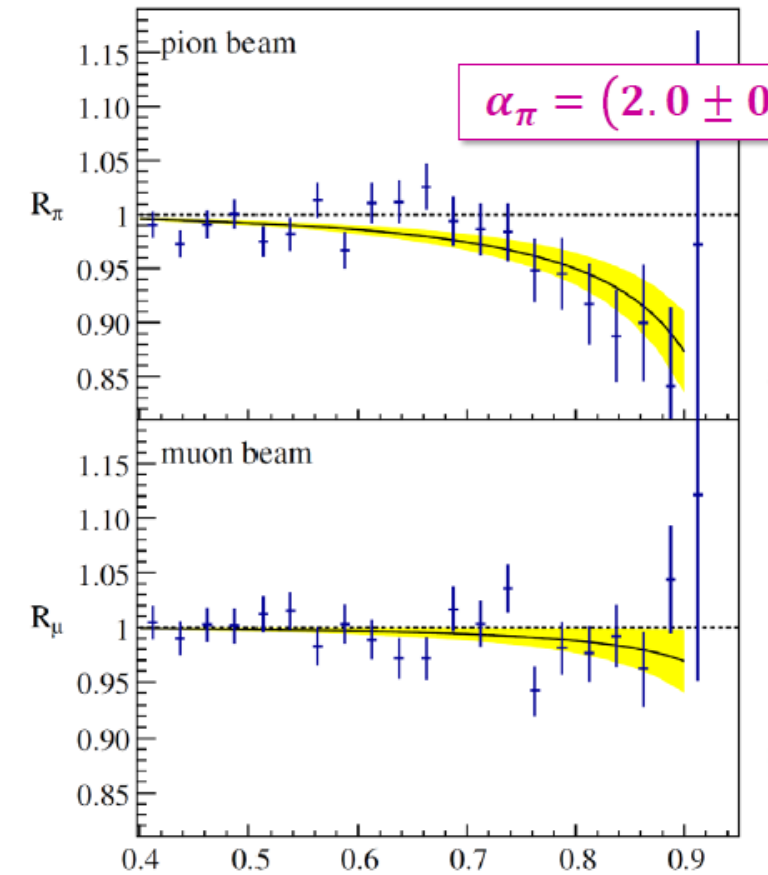
2.4% K^- in the 190 GeV/c
negative hadron beam.
(CEDAR)



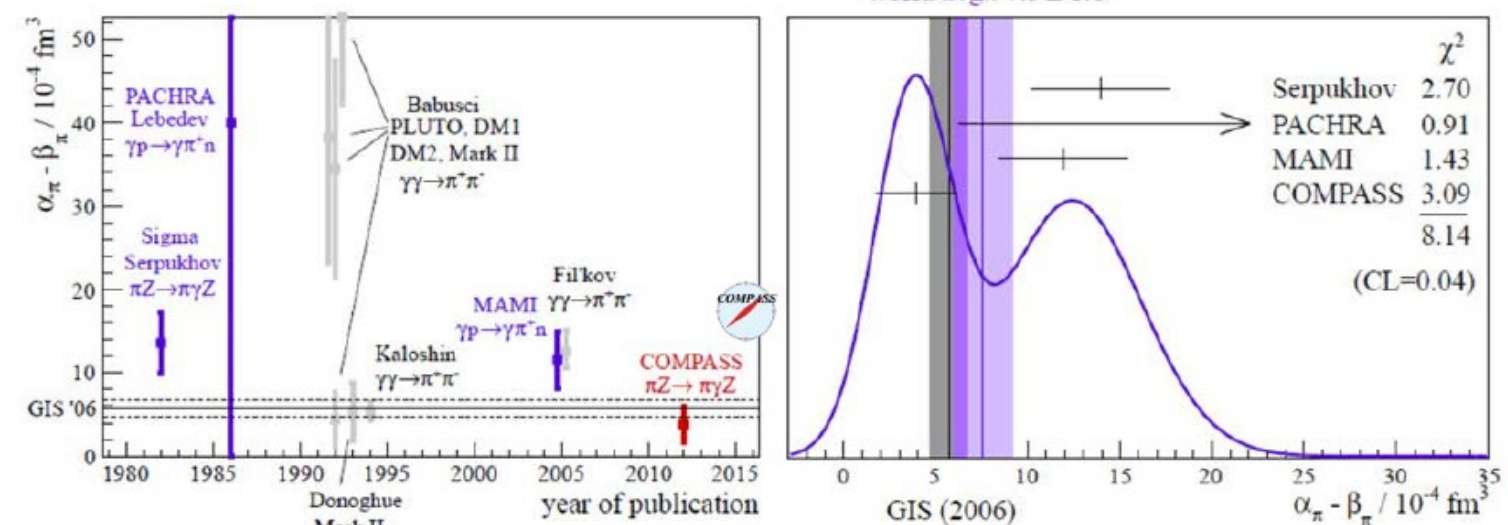
We have 720 000 exclusive $K^- \pi^- \pi^+$ events
in the range $1:0 < m_{K\pi\pi} < 3:0 \text{ GeV}/c^2$
and $0:1 < t' < 1:0 (\text{GeV}/c)^2$.



PRL 114 (2015) 062002

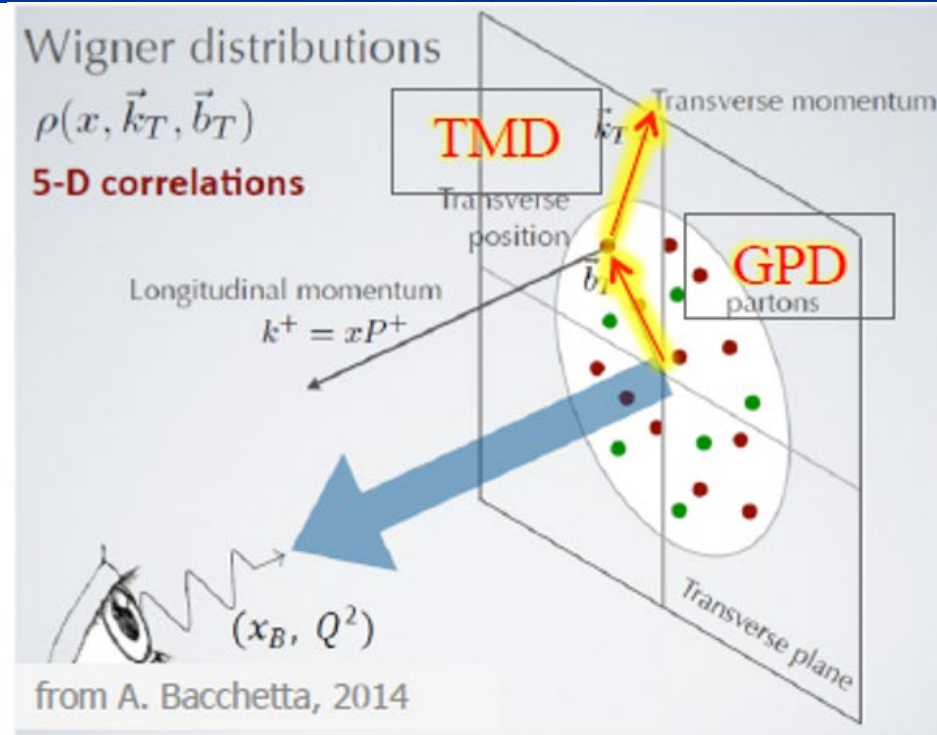


world data including COMPASS

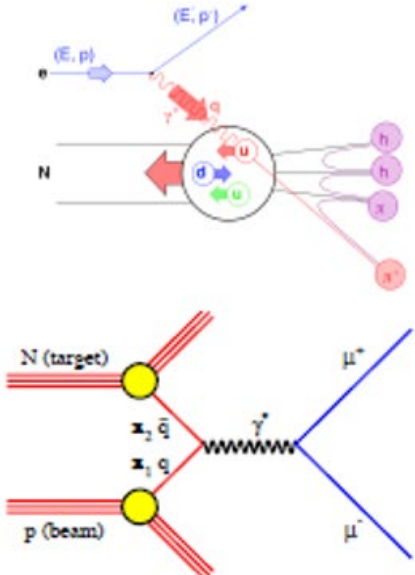


the COMPASS result is in significant tension with the earlier measurements

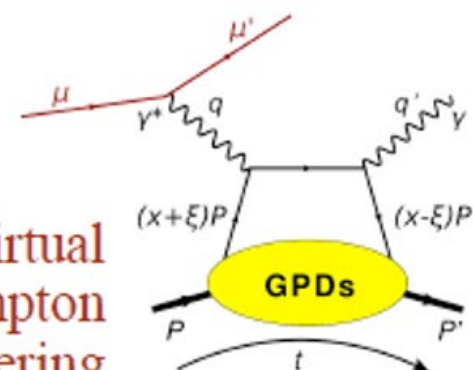
the expectation from ChPT is confirmed within the uncertainties



Semi-Inclusive DIS



Drell-Yan process



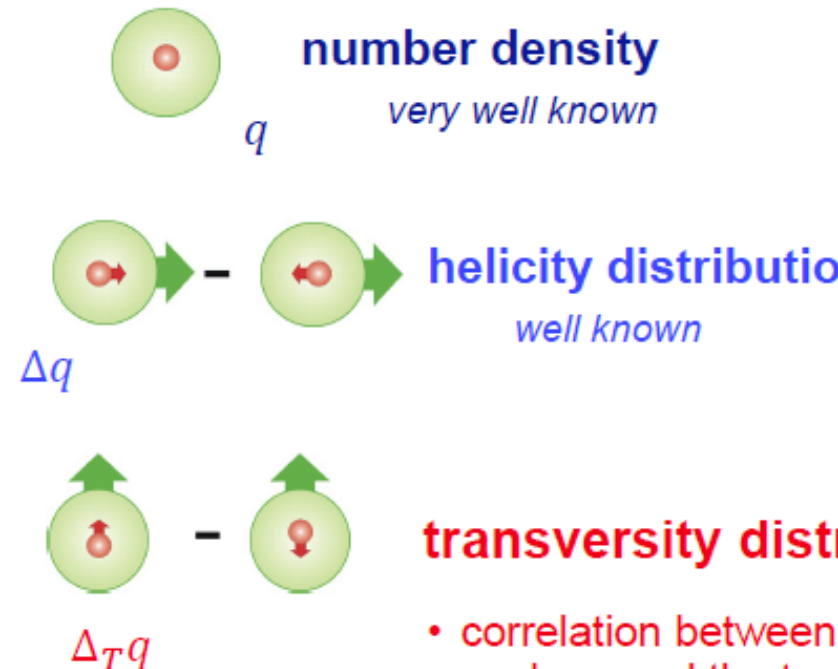
Deeply Virtual Compton Scattering

Transversity Momentum Distributions: **TMD** (x, k_T):
 probe the **transverse parton momentum** dependence

Generalized Parton Distributions : **GPD** (x, b_T):
 probe the **transverse parton distance** dependence

COMPASS explores the multi dimensional structure of the nucleon both in momentum and in configuration space, via SIDIS, D-Y and DVCS/DVMP

collinear description leading twist



		nucleon polarisation		
		U	L	T
quark polarisation	U	f_1		
	L		g_1	
	T			h_1

transversity distribution

- correlation between the transverse polarisation of the nucleon and the transverse polarisation of the quark
- a chirally-odd distribution, not observable in DIS
- related to **tensor charge**
- first experimental evidence in 2005

taking into account the quark intrinsic transverse momentum k_T , at leading order
8 TMD PDFs are needed for a full description of the nucleon structure

correlations between parton transverse
momentum, parton spin and nucleon spin

SIDIS gives access to all of them

		nucleon polarisation	
		U	L
quark polarisation	U	f_1	
	L		g_1
T	h_1^\perp	h_{1L}^\perp	h_1 h_{1T}^\perp

h_1

f_{1T}^\perp Sivers PDF

*correlation between the transverse polarization
of the nucleon and the transverse momentum
of the partons*

$$\begin{aligned}
& \frac{d\sigma}{dx dy d\psi dz d\phi_h dP_{h\perp}^2} = \\
& \frac{\alpha^2}{xy Q^2} \frac{y^2}{2(1-\varepsilon)} \left(1 + \frac{\gamma^2}{2x}\right) \left\{ F_{UU,T} + \varepsilon F_{UU,L} + \sqrt{2\varepsilon(1+\varepsilon)} \cos \phi_h F_{UU}^{\cos \phi_h} \right. \\
& + \varepsilon \cos(2\phi_h) F_{UU}^{\cos 2\phi_h} + \lambda_e \sqrt{2\varepsilon(1-\varepsilon)} \sin \phi_h F_{LU}^{\sin \phi_h} \\
& + S_{\parallel} \left[\sqrt{2\varepsilon(1+\varepsilon)} \sin \phi_h F_{UL}^{\sin \phi_h} + \varepsilon \sin(2\phi_h) F_{UL}^{\sin 2\phi_h} \right] + S_{\parallel} \lambda_e \left[\sqrt{1-\varepsilon^2} F_{LL} + \sqrt{2\varepsilon(1-\varepsilon)} \cos \phi_h F_{LL}^{\cos \phi_h} \right] \\
& + |\mathbf{S}_{\perp}| \left[\sin(\phi_h - \phi_S) \left(F_{UT,T}^{\sin(\phi_h - \phi_S)} + \varepsilon F_{UT,L}^{\sin(\phi_h - \phi_S)} \right) \right. \\
& + \varepsilon \sin(\phi_h + \phi_S) F_{UT}^{\sin(\phi_h + \phi_S)} + \varepsilon \sin(3\phi_h - \phi_S) F_{UT}^{\sin(3\phi_h - \phi_S)} \\
& \left. + \sqrt{2\varepsilon(1+\varepsilon)} \sin \phi_S F_{UT}^{\sin \phi_S} + \sqrt{2\varepsilon(1+\varepsilon)} \sin(2\phi_h - \phi_S) F_{UT}^{\sin(2\phi_h - \phi_S)} \right] \\
& + |\mathbf{S}_{\perp}| \lambda_e \left[\sqrt{1-\varepsilon^2} \cos(\phi_h - \phi_S) F_{LT}^{\cos(\phi_h - \phi_S)} + \sqrt{2\varepsilon(1-\varepsilon)} \cos \phi_S F_{LT}^{\cos \phi_S} \right. \\
& \left. + \sqrt{2\varepsilon(1-\varepsilon)} \cos(2\phi_h - \phi_S) F_{LT}^{\cos(2\phi_h - \phi_S)} \right] \right\},
\end{aligned}$$

14 independent azimuthal modulations

$$\begin{aligned}
 \frac{d\sigma}{dx dy d\psi dz d\phi_h dP_{h\perp}^2} = & \\
 & \frac{\alpha^2}{xyQ^2} \frac{y^2}{2(1-\varepsilon)} \left(1 + \frac{\gamma^2}{2x}\right) \left\{ F_{UU,T} + \varepsilon F_{UU,L} + \sqrt{2\varepsilon(1+\varepsilon)} \cos \phi_h F_{LU} \right. \\
 & \quad \left. h_i^\perp H_i^\perp \right\} \\
 & + \varepsilon \cos(2\phi_h) F_{UU}^{\cos 2\phi_h} + \lambda_e \sqrt{2\varepsilon(1-\varepsilon)} \sin \phi_h F_{LU}^{\sin \phi_h} \\
 & + S_\parallel \left[\sqrt{2\varepsilon(1+\varepsilon)} \sin \phi_h F_{UL}^{\sin \phi_h} + \varepsilon \sin(2\phi_h) F_{UL}^{\sin 2\phi_h} \right] + S_\parallel \lambda_e \left[\sqrt{1-\varepsilon^2} F_{LL} + \sqrt{2\varepsilon(1-\varepsilon)} \cos \phi_h F_{LL}^{\cos \phi_h} \right] \\
 & + |S_\perp| \left[\sin(\phi_h - \phi_S) \left(F_{UT,T}^{\sin(\phi_h - \phi_S)} + \varepsilon F_{UT,L}^{\sin(\phi_h - \phi_S)} \right) \right. \\
 & \quad \left. h_i^\perp H_i^\perp \right] \\
 & + \varepsilon \left[\sin(\phi_h + \phi_S) F_{UT}^{\sin(\phi_h + \phi_S)} + \varepsilon \sin(3\phi_h - \phi_S) F_{UT}^{\sin(3\phi_h - \phi_S)} \right] \\
 & \quad \left. h_i^\perp H_i^\perp \right] \\
 & + \sqrt{2\varepsilon(1+\varepsilon)} \sin \phi_S F_{UT}^{\sin \phi_S} + \sqrt{2\varepsilon(1+\varepsilon)} \sin(2\phi_h - \phi_S) F_U^{\sin(2\phi_h - \phi_S)} \\
 & + |S_\perp| \lambda_e \left[\sqrt{1-\varepsilon^2} \cos(\phi_h - \phi_S) F_{LT}^{\cos(\phi_h - \phi_S)} + \sqrt{2\varepsilon(1-\varepsilon)} \cos \phi_h F_{LU}^{\cos \phi_h} \right. \\
 & \quad \left. g_i^\perp D_i \right] \\
 & + \sqrt{2\varepsilon(1-\varepsilon)} \cos(2\phi_h - \phi_S) F_{LT}^{\cos(2\phi_h - \phi_S)} \Big\},
 \end{aligned}$$

leading twist amplitudes
 → convolutions of the
 transversity and
 TMD PDFs and FFs

SIDIS

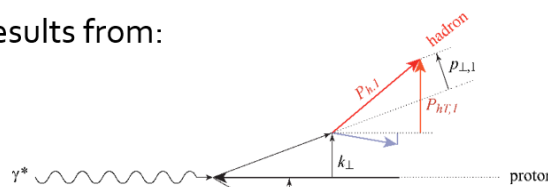
- allows to disentangle the effects related to the different TMD PDFs and to access all of them
- by identifying the final state hadrons and using different targets allows for flavour separation

→ very powerful tool

ALL modulations measured by COMPASS

- The cross-section dependence from P_{hT} results from:

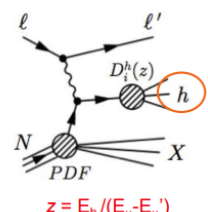
- intrinsic k_\perp of the quarks
- p_\perp generated in the quark fragmentation



- The azimuthal modulations in the unpolarised cross sections comes from:

- Intrinsic k_\perp of the quarks
- The Boer-Mulders PDF

→ Measure hadron multiplicities in SIDIS: $\mu^+ d \rightarrow \mu^+ h^\pm X$ $h = \pi, K, p$

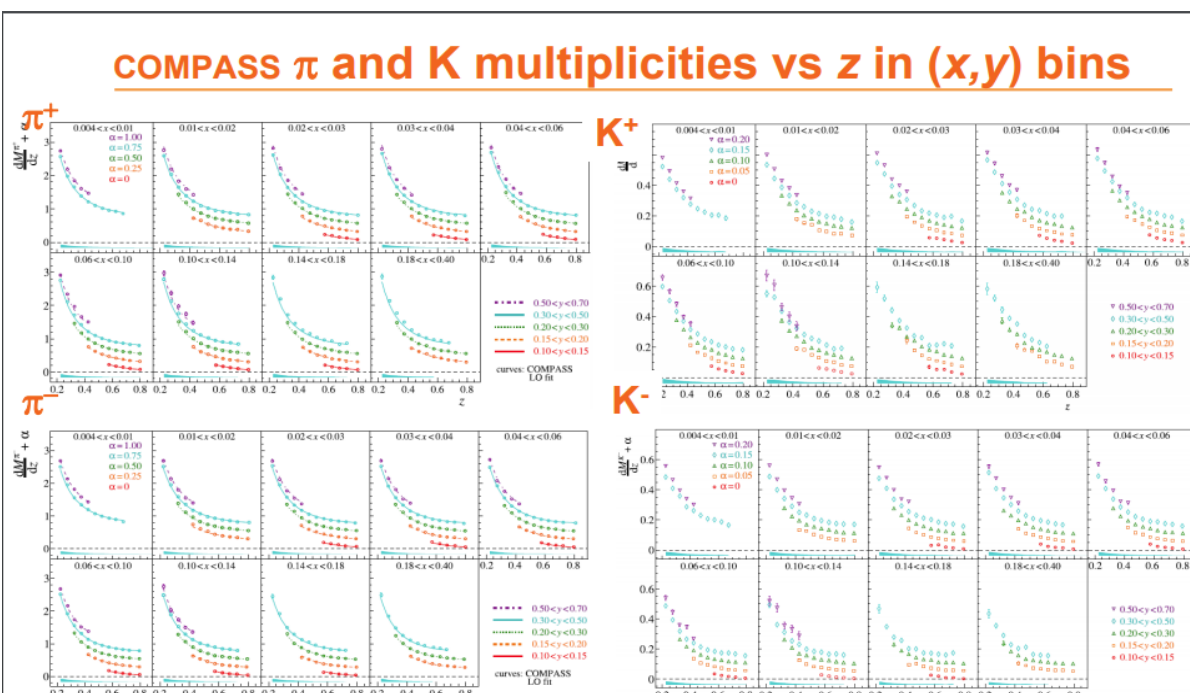


$$\frac{dM^h(x, Q^2, z)}{dz} \text{ at LO} = \sum_q e_q^2 f_q(x, Q^2) D_q^h(z, Q^2)$$

PDFs depend on x , while FFs depend on z

→ With kaons, access typically : $s(x, Q^2) \cdot D_s^K(z, Q^2)$

π and K multiplicities constitute an input to global NLO QCD analyses to extract quark FFs

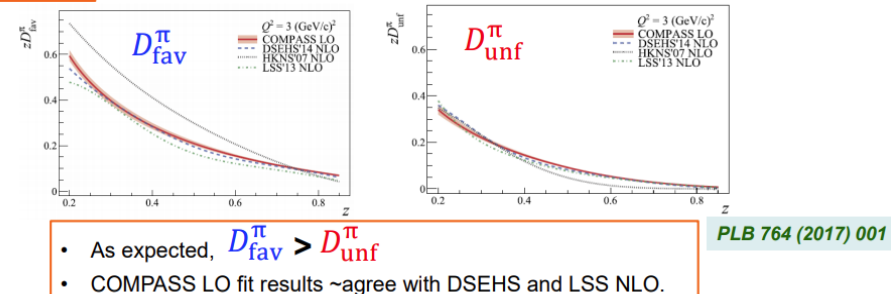


- Isoscalar target (${}^6\text{LiD}$)
- More than 1200 points in total, various Q^2 staggered vertically for clarity
- Strong z dependence
- $M(\pi^+) \sim M(\pi^-)$ and $M(K^+) > M(K^-)$

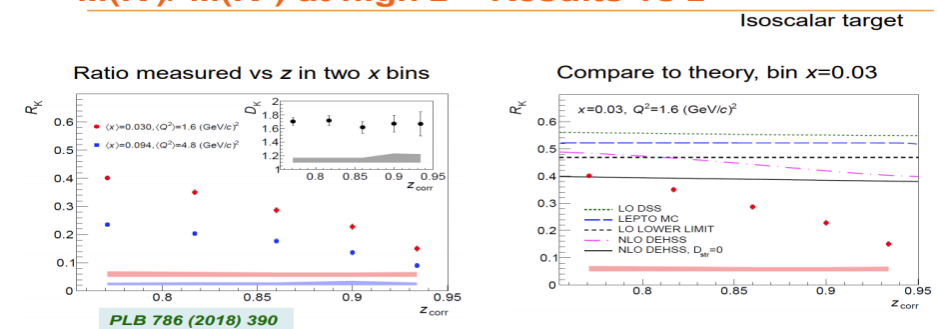
PLB 764 (2017) 001
PLB 767 (2017) 133

From multiplicities to quark Fragmentation Functions

Pions Results from COMPASS LO fits assuming 2 independent FFs: D_{fav}^π D_{unf}^π



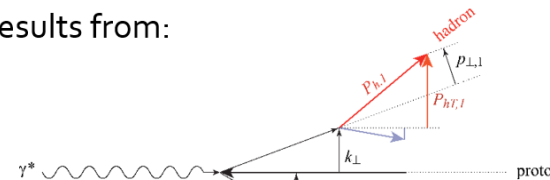
$M(K^-)/M(K^+)$ at high z – Results vs z



$M(K^-) / M(K^+)$ ratio well below expectations at high z

- The cross-section dependence from P_{hT} results from:

- intrinsic k_\perp of the quarks
- p_\perp generated in the quark fragmentation



- The azimuthal modulations in the unpolarised cross sections comes from:

- Intrinsic k_\perp of the quarks
- The Boer-Mulders PDF

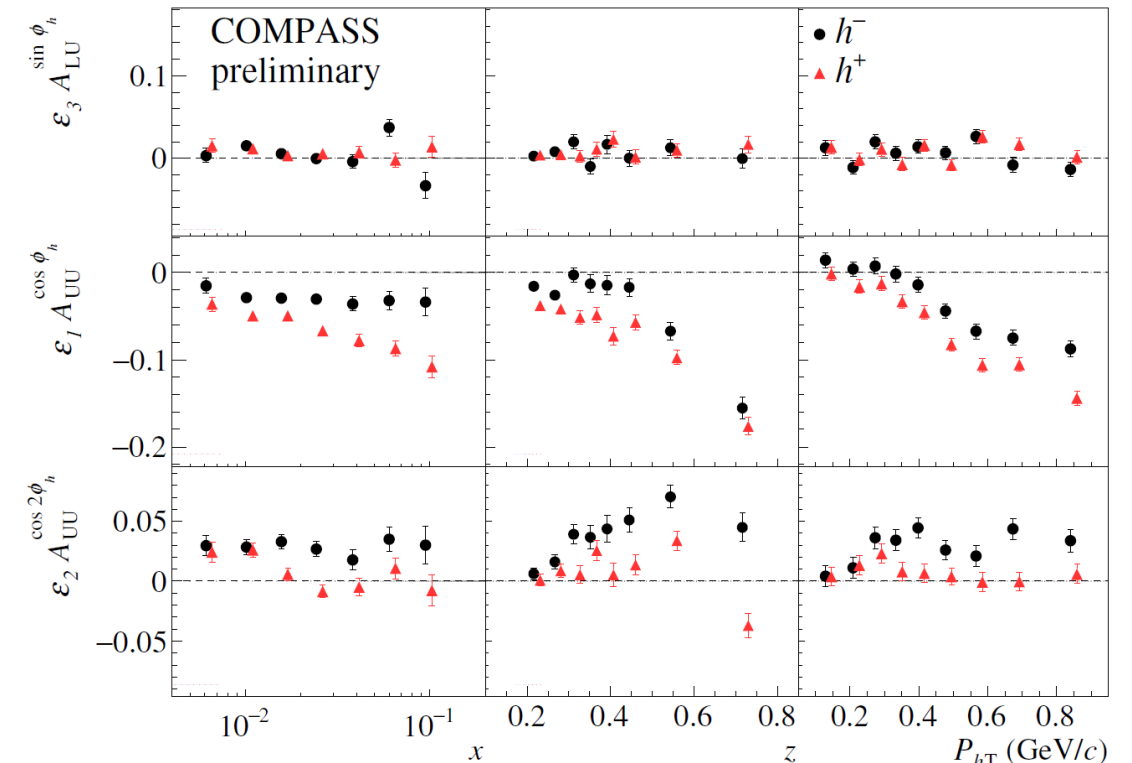
When looking at the content of the structure functions/modulations in terms of TMD PDFs for the $\cos \phi_h$ and $\cos 2\phi_h$ we can write:

$$F_{UU}^{\cos \phi_h} = -\frac{2M}{Q} C \left[\frac{\hat{h} \cdot \vec{k}_\perp}{M} f_1 D_1 - \frac{p_\perp k_\perp}{M} \frac{\vec{P}_{hT} - z(\hat{h} \cdot \vec{k}_\perp)}{z M_h M} h_1^\perp H_1^\perp \right] + \text{twists} > 3$$

$$F_{UU}^{\cos 2\phi_h} = C \left[\frac{(\hat{h} \cdot \vec{k}_\perp)(\hat{h} \cdot \vec{p}_\perp) - \vec{p}_\perp \cdot \vec{k}_\perp}{MM_h} h_1^\perp H_1^\perp \right] + \text{twists} > 3$$

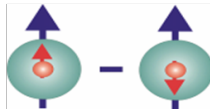
In the $\cos 2\phi_h$ Cahn effects enters only at twist 4

$$F_{\text{Cahn}}^{\cos 2\phi_h} \approx \frac{2}{Q^2} C \left[\left\{ 2(\hat{h} \cdot \vec{k}_\perp)^2 - k_\perp^2 \right\} f_1 D_1 \right]$$



Strong kinematic dependences

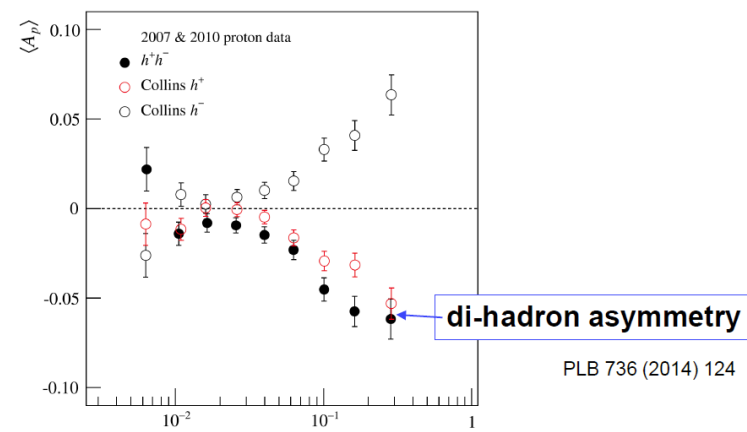
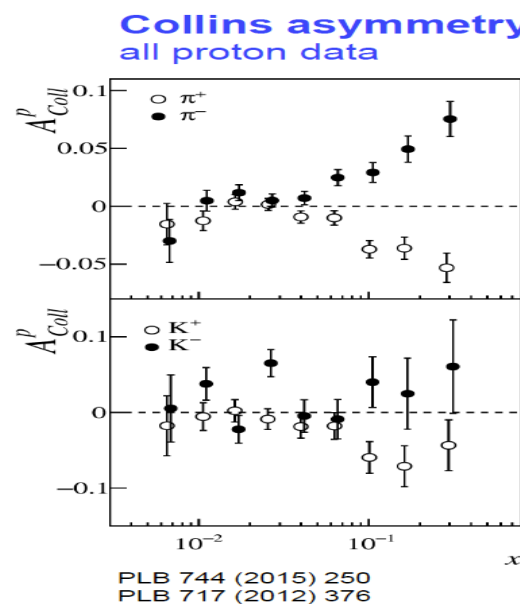
$$h_1^q(x) = q^{\uparrow\uparrow}(x) - q^{\uparrow\downarrow}(x)$$



$q = u_\nu, d_\nu, q_{\text{sea}}$
quark with spin parallel to the nucleon spin in a transversely polarised nucleon

- probes the relativistic nature of quark dynamics
- no contribution from the gluons \rightarrow simple Q^2 evolution
- Positivity: Soffer bound..... $2|h_1^q| \leq f_1^q + g_1^q$ *Soffer, PRL 74 (1995)*
- first moments: tensor charge..... $\delta q(Q^2) = \int_0^1 dx [h_1^q(x) - h_1^{\bar{q}}(x)]$
- is chiral-odd: decouples from inclusive DIS

Bakker; Leader, Truemmer, PRD 70 (04)



study of the interplay between
Collins and di-hadron asymmetries
– not independent

PLB 753 (2016) 406

observable effects are given only by the
product of $h_1^q(x)$ and an other chiral-odd function
can be measured in SIDIS on a transversely polarised target
via “quark polarimetry”



“Collins” asymmetry

“Collins” Fragmentation Function

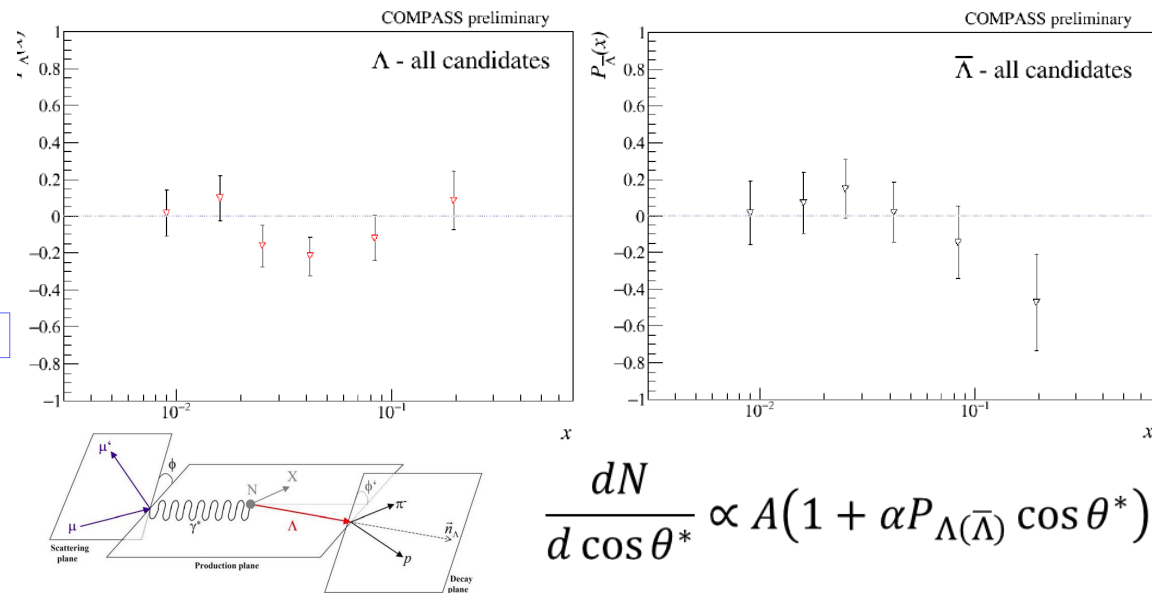
“two-hadron” asymmetry

“Interference” Fragmentation Function

Λ polarisation

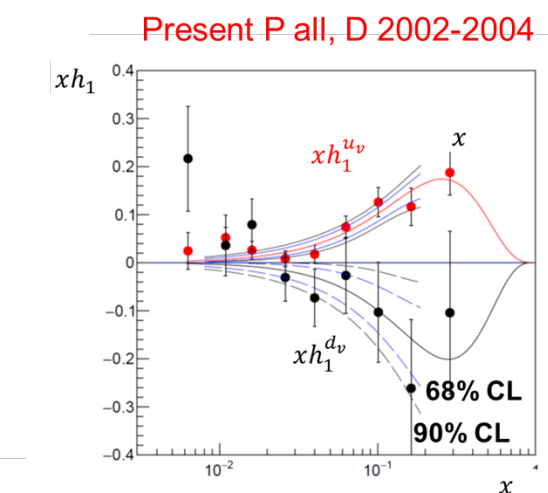
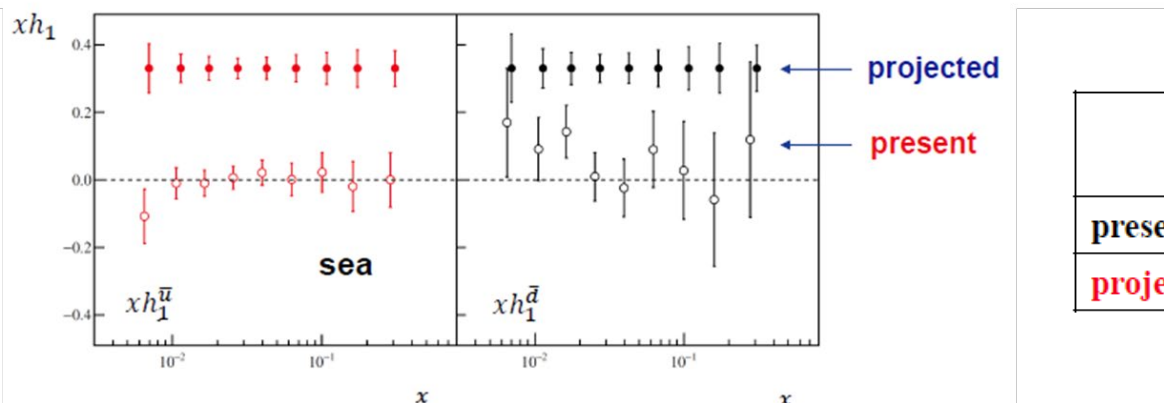
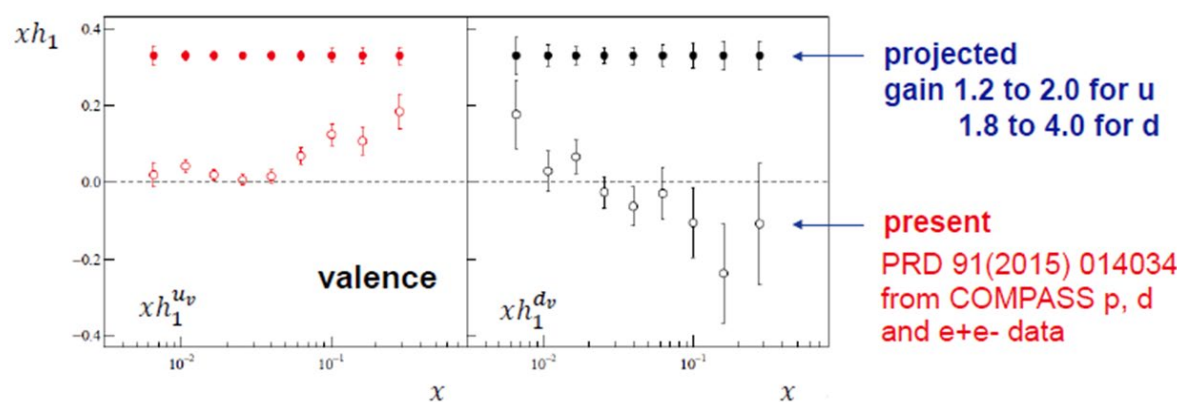
measured for the first time

Fragmentation Function of $q \uparrow \rightarrow \Lambda$

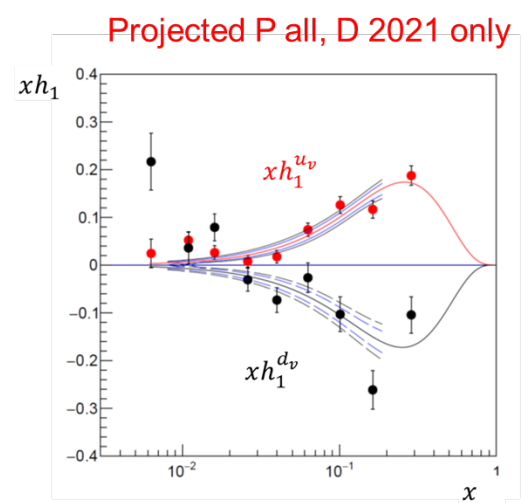


One year of run with 160 GeV muons to measure SIDIS off transversely polarised d the missing measurement to complete the COMPASS exploratory programme collecting the same statistics as in 2010,

The deuteron asymmetries will have a statistical uncertainty $\sigma_d \cong 0.6 \sigma_p^{2010}$

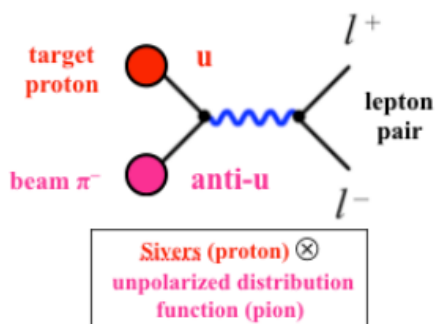


	$\delta_u = \int_{\Omega_x} dx h_1^u(x)$	$\delta_d = \int_{\Omega_x} dx h_1^d(x)$	$g_T = \delta_u - \delta_d$
present	0.201 ± 0.032	-0.189 ± 0.108	0.390 ± 0.087
projected	0.201 ± 0.019	-0.189 ± 0.040	0.390 ± 0.044



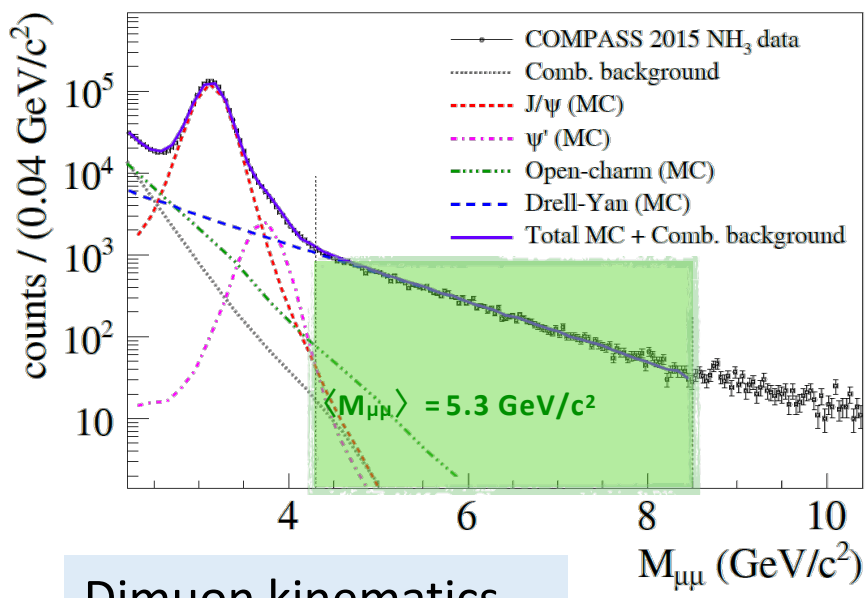
$$\Omega_x: 0.008 \div 0.210$$

Drell-Yan

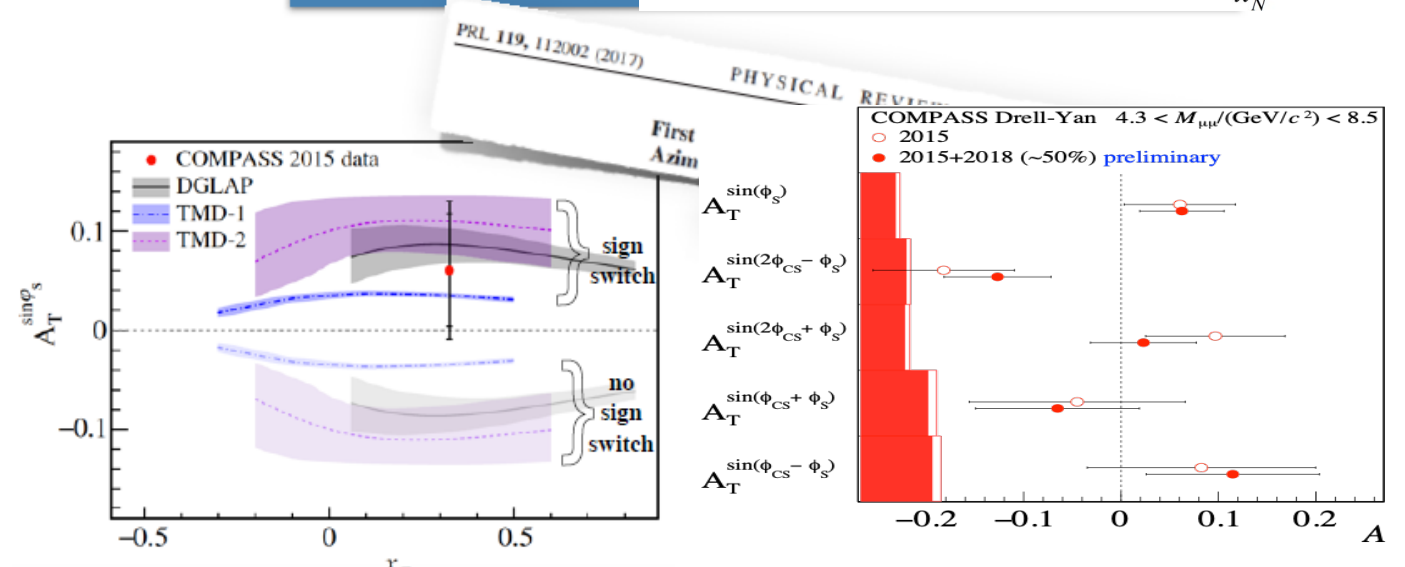
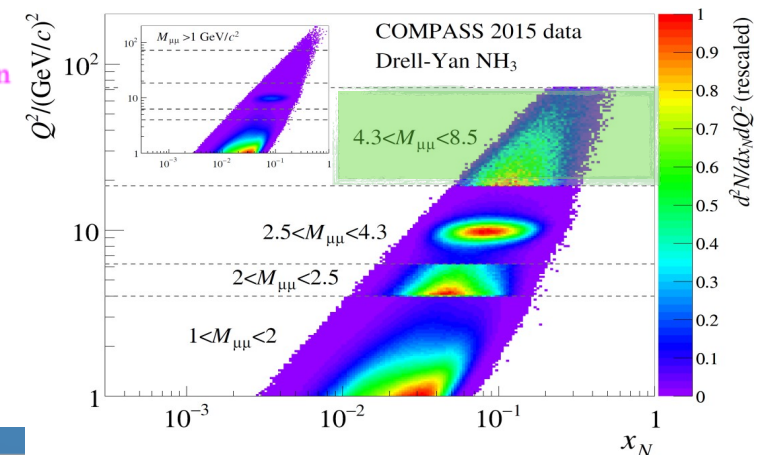
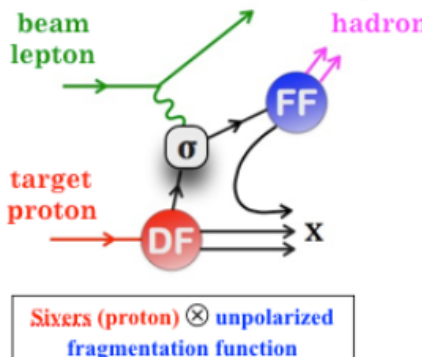


The **Sivers** TMD is expected to have the **same magnitude**, but **opposite sign** in SIDIS vs. DY. The same applies to the **Boer-Mulders** function.

Crucial test of TMD framework.

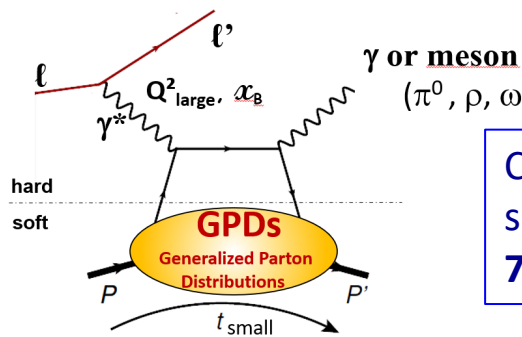


Semi-Inclusive Deep-Inelastic Scattering



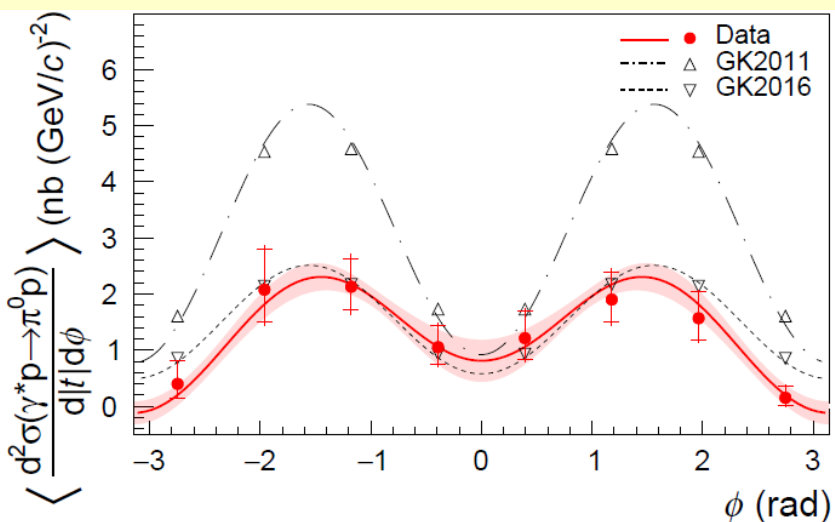
"DGLAP" M. Anselmino, M. Boglione, U. D'Alesio, F. Murgia, and A. Prokudin, J. High Energy Phys. 04 (2017) 046.
 "TMD 1" M. G. Echevarria, A. Idilbi, Z.-B. Kang, and I. Vitev, Phys. Rev. D 89, 074013 (2014).
 "TMD 2" P. Sun and F. Yuan, Phys. Rev. D 88, 114012 (2013).

COMPASS 2012 data



COMPASS DVCS cross sections published: PLB
793 (2019) 188;

PLB 805 (2020) 135454, hep-ex/1903.12030

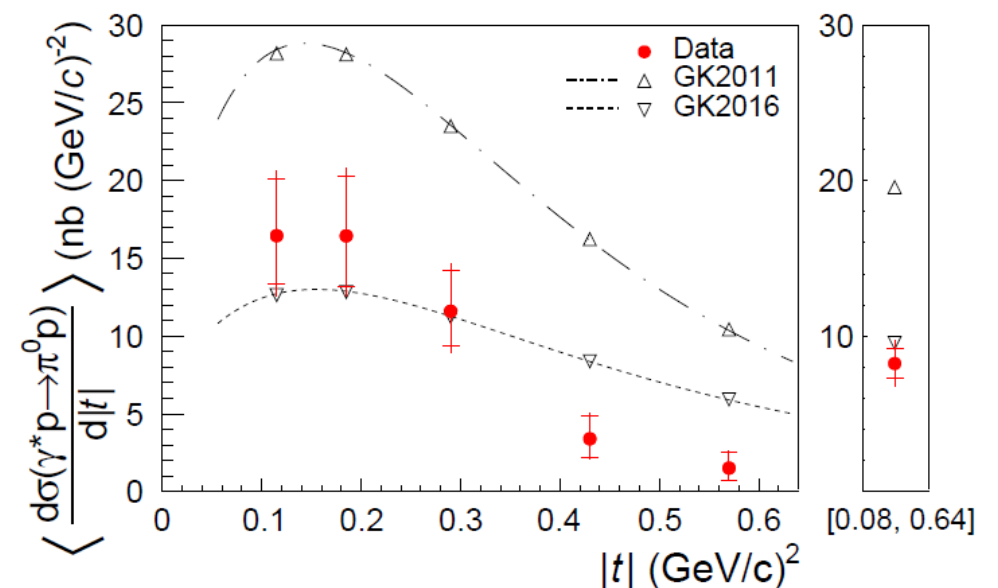


Σ_L depends on H , E : leading twist contribution \rightarrow should be dominant.

surprisingly Σ_T , Σ_{TT} , Σ_{LT} involving also H_T and E_T are found to be large

$$\mu p \rightarrow \mu \pi^0 p$$

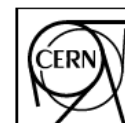
$$\frac{d^2\sigma}{dt d\phi_\pi} = \frac{1}{2\pi} \left[\left(\frac{d\sigma_T}{dt} + \epsilon \frac{d\sigma_L}{dt} \right) + \epsilon \cos 2\phi_\pi \frac{d\sigma_{TT}}{dt} + \sqrt{2\epsilon(1+\epsilon)} \cos \phi_\pi \frac{d\sigma_{LT}}{dt} \right]$$



Goloskokov-Kroll

COMPASS++/AMBER: a New QCD Facility at CERN SPS

EUROPEAN ORGANIZATION FOR NUCLEAR RESEARCH



CERN-SPSC-2019-003
SPSC-I-250
January 25, 2019

<http://arxiv.org/abs/1808.00848>

Apparatus for Meson and Baryon Experimental Research
> 270 authors

Letter of Intent:
A New QCD facility at the M2 beam line of the CERN SPS*
COMPASS++[†]/AMBER[‡]

B. Adams^{13,12}, C.A. Aidala¹, R. Akhunzyanov¹⁴, G.D. Alexeev¹⁴, M.G. Alexeev⁴¹, A. Amoroso^{41,42},

[hep-ex] 25 Jan 2019

Program	Physics Goals	Beam Energy [GeV]	Beam Intensity [s^{-1}]	Trigger Rate [kHz]	Beam Type	Target	Earliest start time, duration	Hardware additions
muon-proton elastic scattering	Precision proton-radius measurement	100	$4 \cdot 10^6$	100	μ^\pm	high-pressure H ₂	2022 1 year	active TPC, SciFi trigger, silicon veto,
Hard exclusive reactions	GPD E	160	$2 \cdot 10^7$	10	μ^\pm	NH ₃ [†]	2022 2 years	recoil silicon, modified polarised target magnet
Input for Dark Matter Search	\bar{p} production cross section	20-280	$5 \cdot 10^5$	25	p	LH ₂ , LHe	2022 1 month	liquid helium target
\bar{p} -induced spectroscopy	Heavy quark exotics	12, 20	$5 \cdot 10^7$	25	\bar{p}	LH ₂	2022 2 years	target spectrometer: tracking, calorimetry
Drell-Yan	Pion PDFs	190	$7 \cdot 10^7$	25	π^\pm	C/W	2022 1-2 years	
Drell-Yan (RF)	Kaon PDFs & Nucleon TMDs	~100	10^8	25-50	K^\pm, \bar{p}	NH ₃ [†] , C/W	2026 2-3 years	"active absorber", vertex detector
Primakoff (RF)	Kaon polarisability & pion life time	~100	$5 \cdot 10^6$	> 10	K^-	Ni	non-exclusive 2026 1 year	
Prompt Photons (RF)	Meson gluon PDFs	≥ 100	$5 \cdot 10^6$	10-100	K^\pm, π^\pm	LH ₂ , Ni	non-exclusive 2026 1-2 years	hodoscope
K -induced Spectroscopy (RF)	High-precision strange-meson spectrum	50-100	$5 \cdot 10^6$	25	K^-	LH ₂	2026 1 year	recoil TOF, forward PID
Vector mesons (RF)	Spin Density Matrix Elements	50-100	$5 \cdot 10^6$	10-100	K^\pm, π^\pm	from H to Pb	2026 1 year	

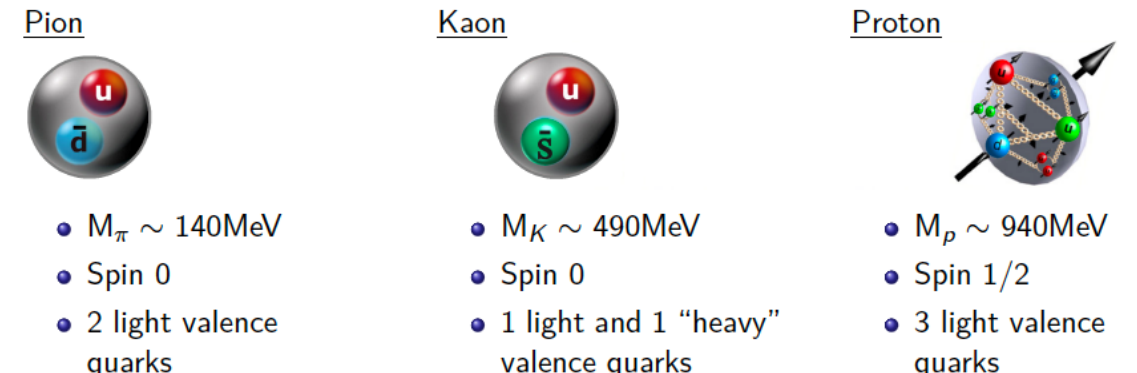
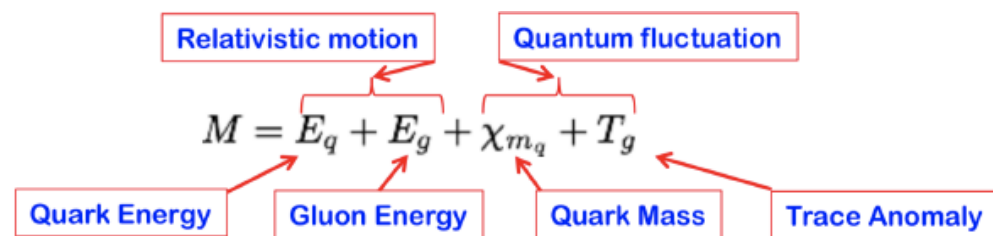
Table 2: Requirements for future programmes at the M2 beam line after 2021. Muon beams are in blue, conventional hadron beams in green, and RF-separated hadron beams in red.

How does the all visible matter in the universe come about and what defines its mass scale?

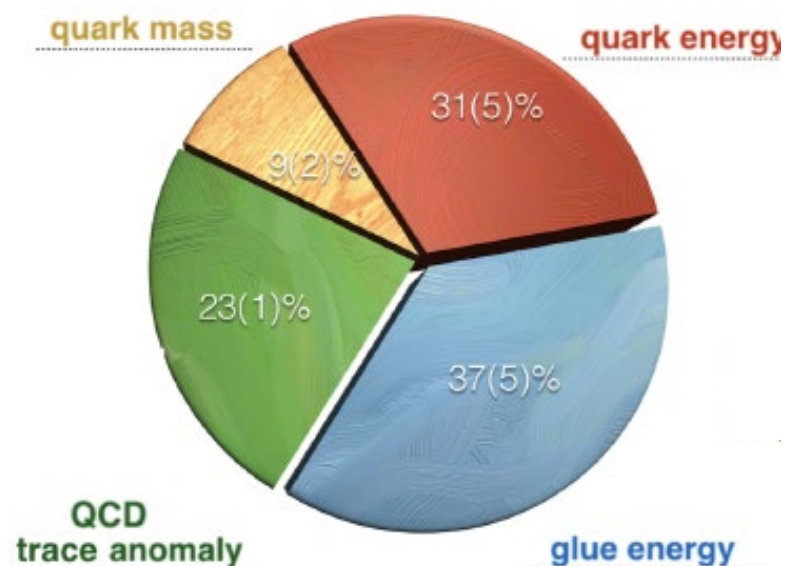
The Higgs-boson does NOT help to answer this question.

- ✓ The Higgs-boson mechanism produces only a small fraction of all visible mass
- ✓ The Higgs-generated mass scales explain neither the “huge” proton mass nor the ‘nearly-masslessness’ of the pion

One of the possible proton mass decomposition (calculation on lattice)
 Yi-Bo Yang et al., Phys.Rev.Lett. 121 (2018) no.21, 212001



Higgs generated masses of the valence quarks:
 $M_{(u+d)} \sim 7\text{ MeV}$ $M_{(u+s)} \sim 100\text{ MeV}$ $M_{(u+u+d)} \sim 10\text{ MeV}$



Program	Physics Goals	Beam Energy [GeV]	Beam Intensity [s^{-1}]	Trigger Rate [kHz]	Beam Type	Target	Earliest start time, duration	Hardware additions
muon-proton elastic scattering	Precision proton-radius measurement	100	$4 \cdot 10^6$	100	μ^\pm	high-pressure H ₂	2022 1 year	active TPC, SciFi trigger, silicon veto,
Hard exclusive reactions	GPD E	160	$2 \cdot 10^7$	10	μ^\pm	NH ₃ [†]	2022 2 years	recoil silicon, modified polarised target magnet
Input for Dark Matter Search	\bar{p} production cross section	20-280	$5 \cdot 10^5$	25	p	LH ₂ , LHe	2022 1 month	liquid helium target
\bar{p} -induced spectroscopy	Heavy quark exotics	12, 20	$5 \cdot 10^7$	25	\bar{p}	LH ₂	2022 2 years	target spectrometer: tracking, calorimetry
Drell-Yan	Pion PDFs	190	$7 \cdot 10^7$	25	π^\pm	C/W	2022 1-2 years	
Drell-Yan (RF)	Kaon PDFs & Nucleon TMDs	~100	10^8	25-50	K^\pm, \bar{p}	NH ₃ [†] , C/W	2026 2-3 years	"active absorber", vertex detector
Primakoff (RF)	Kaon polarisability & pion life time	~100	$5 \cdot 10^6$	> 10	K^-	Ni	non-exclusive 2026 1 year	
Prompt Photons (RF)	Meson gluon PDFs	≥ 100	$5 \cdot 10^6$	10-100	K^\pm, π^\pm	LH ₂ , Ni	non-exclusive 2026 1-2 years	hodoscope
K -induced Spectroscopy (RF)	High-precision strange-meson spectrum	50-100	$5 \cdot 10^6$	25	K^-	LH ₂	2026 1 year	recoil TOF, forward PID
Vector mesons (RF)	Spin Density Matrix Elements	50-100	$5 \cdot 10^6$	10-100	K^\pm, π^\pm	from H to Pb	2026 1 year	

Table 2: Requirements for future programmes at the M2 beam line after 2021. Muon beams are in blue, conventional hadron beams in green, and RF-separated hadron beams in red.

PHASE-1

Conventional **hadron** and **muon** beams

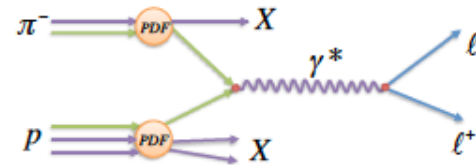
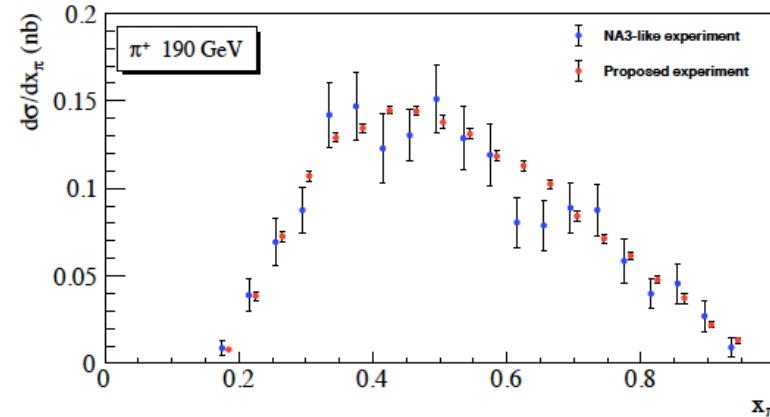
2022 → 2025 and beyond

PHASE-2

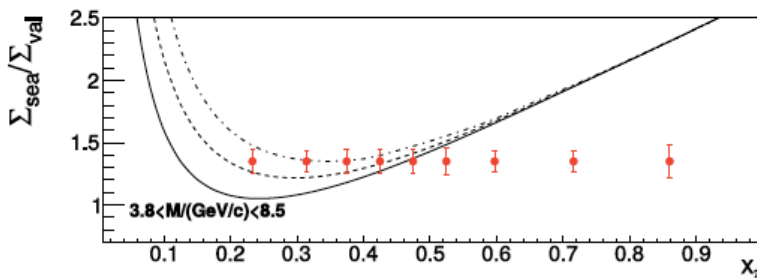
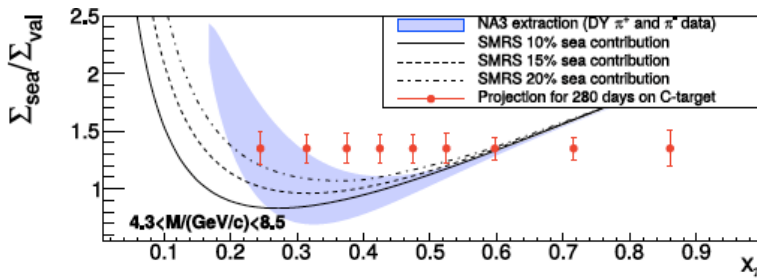
Conventional and RF-separated **Hadron/Hadron** and **muon** beam

2026 and beyond

Pion structure in pion induce DY Expected accuracy as compared to NA3

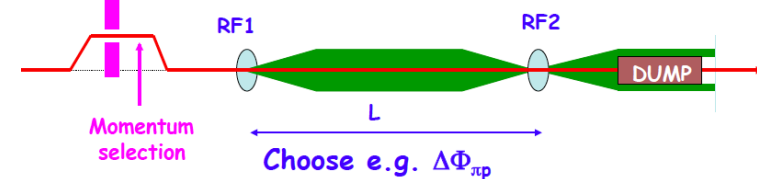


- 90's: NA3, NA10, E615
- 10's: COMPASS-II
- 20's: COMPASS++

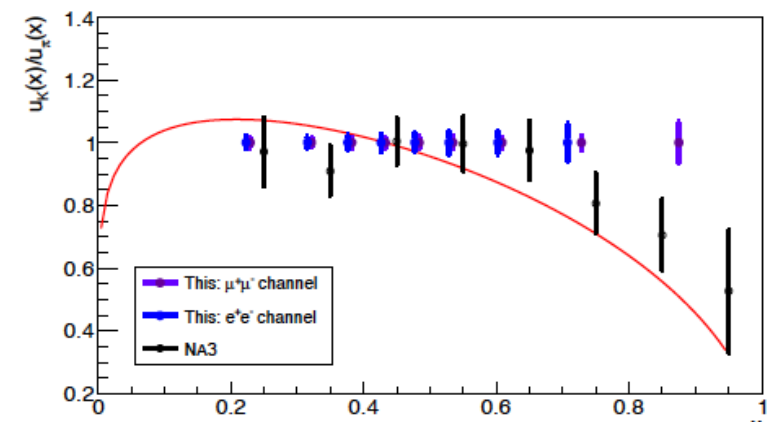


- $\Sigma_V = \sigma^{\pi^- C} - \sigma^{\pi^+ C}$: only valence-valence
- $\Sigma_S = 4\sigma^{\pi^+ C} - \sigma^{\pi^- C}$: no valence-valence
- Collect at least a **factor 10 more** statistics than presently available
- Minimize nuclear effects on target side
 - Projection for 2×140 days of Drell-Yan data taking
 - π^+ to π^- 10:1 time sharing
 - 190 GeV beams on Carbon target ($1.9\lambda_{int}^\pi$)
 - Improvement of shielding to double the intensity is under investigation

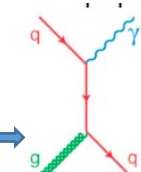
Kaon structure in Kaon induce DY Needs RF separated beam

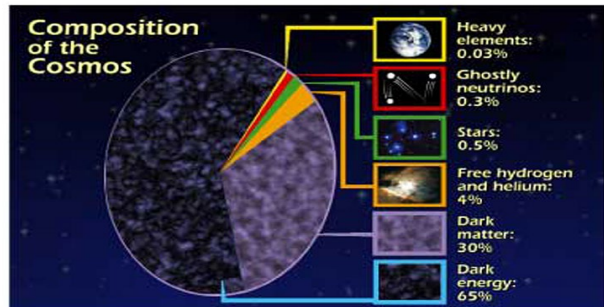


$$\Delta\Phi = 2\pi (L f / c) (\beta_1^{-1} - \beta_2^{-1}) \text{ with } \beta_1^{-1} - \beta_2^{-1} = (m_1^2 - m_2^2)/2p^2$$



To extract pion and kaon pdf,
in particular **gluon pdf**





From the AMS data the antiparticle flux is well known, two type of processes contribute

- SM interaction , protons on the interstellar medium with the production of antiproton
- Antiparticle annihilation

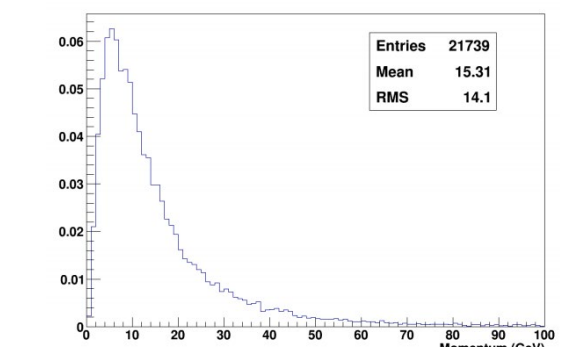
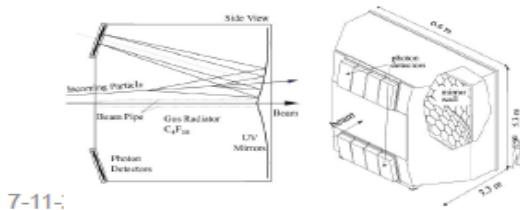


In order to detect a possible excess in the antiparticles flux a good knowledge of the inclusive cross section of p-He interactions

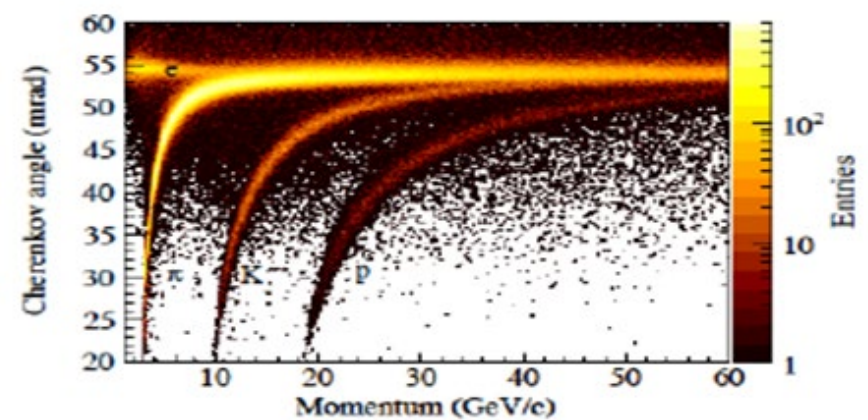
The goal is to measure the inclusive antiproton cross section production in a wide kinematical range with a precision < 10%. C++/AMBER luminosity is a 1000 times

The NA49 one

- Proton beam energy range 50-250 GeV
- Secondary particles identification:
 - Antiprotons (RICH)
 - Positrons and Gamma (ECals)



Momentum spectrum of anti-p produced in p+p interactions at 190 GeV/c

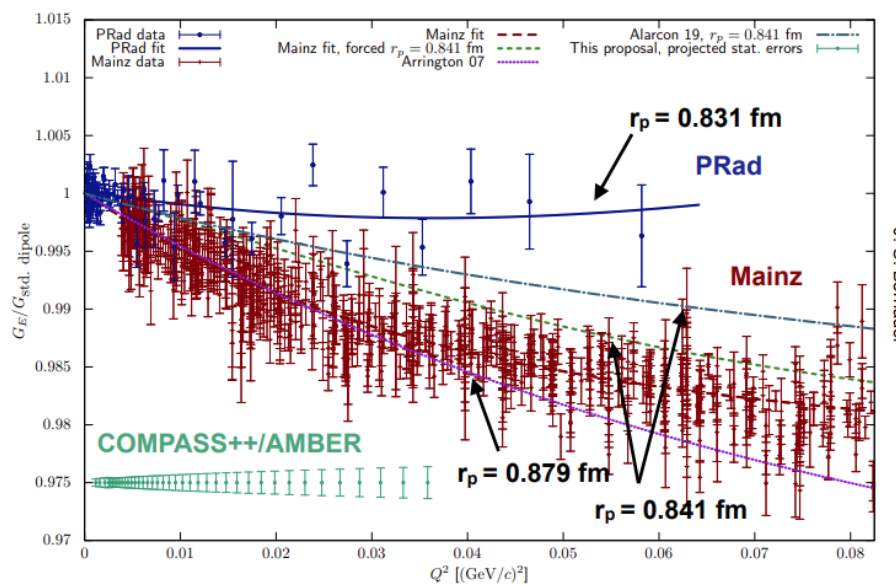
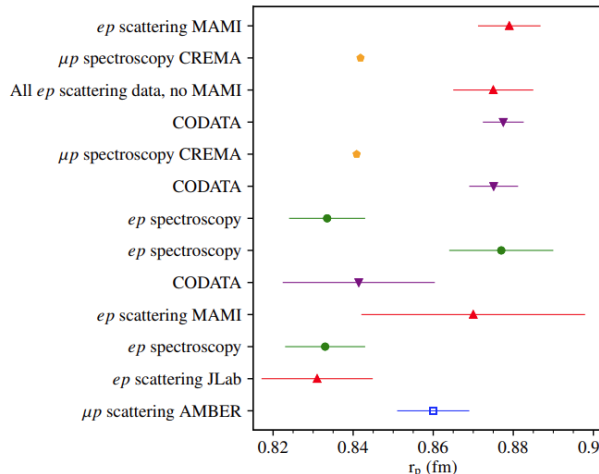


New low momenta is envisaged for the measurement

Data from spectroscopy and e-p scattering

Several experiments with different approaches measured the proton radius with contradicting results.

- Hydrogen spectroscopy:
 - muonic or ordinary hydrogen
 - highest precision using laser spectroscopy
 - favoured value of (0.841 ± 0.001) fm
- Electron-hydrogen scattering:
 - measurement using momentum transfer
 - recent data: MAMI A1 (2010) or JLab (2011)
 - favoured value of (0.879 ± 0.008) fm
 - new in 2019: PRad value of (0.831 ± 0.014) fm
- Two significantly different values obtained
 - the proton-radius puzzle



Cross section, form factor, and the proton charge-radius

Measurement of electric form factor allows to calculate proton charge-radius.

- Electric form-factor G_E defines the proton charge-radius at momentum transfer $Q^2 = 0$:

$$\langle r_p^2 \rangle = -6\hbar^2 \cdot \frac{dG_E(Q^2)}{dQ^2} \Big|_{Q^2=0}$$

- Access to form factors G_E^2 and G_M^2 in Rosenbluth separation of cross section:

$$\frac{d\sigma^{\mu p \rightarrow \mu p}}{dQ^2} = \frac{4\pi\alpha^2}{Q^4} R (\epsilon G_E^2 + \tau G_M^2)$$

$$R = \frac{\vec{p}_\mu^2 - \tau(s - 2m_p^2(1 + \tau))}{\vec{p}_\mu^2(1 + \tau)} \quad \epsilon = \frac{E_\mu^2 - \tau(s - m_\mu^2)}{\vec{p}_\mu^2 - \tau(s - 2m_p^2(1 + \tau))} \quad \tau = \frac{Q^2}{(4m_p^2)}$$

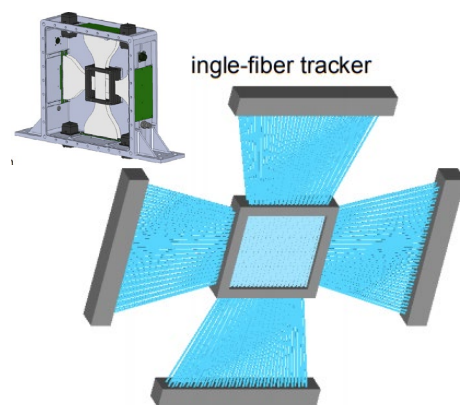
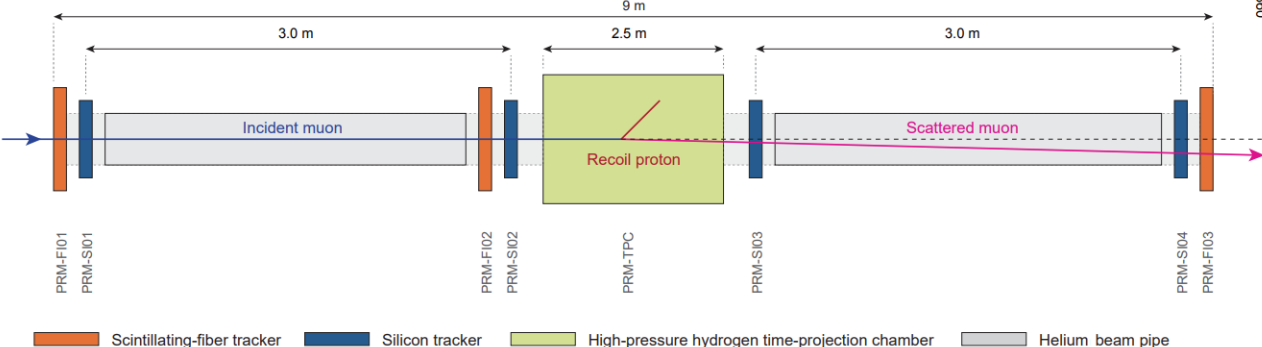
- Suppress magnetic form factor G_M^2
 - Requires $\tau \rightarrow 0$
 - Measurement at low- Q^2 values of $\mathcal{O}(10^{-2})$
- Measurement at high-energy $\mathcal{O}(10 - 100)$ GeV
 - Results in $\epsilon \rightarrow 1$
 - Cross-section directly proportional to G_E^2

The Proton-Radius Puzzle: new hardware requirements

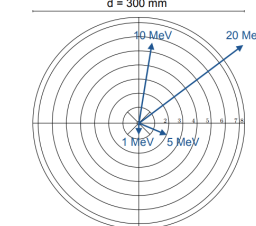
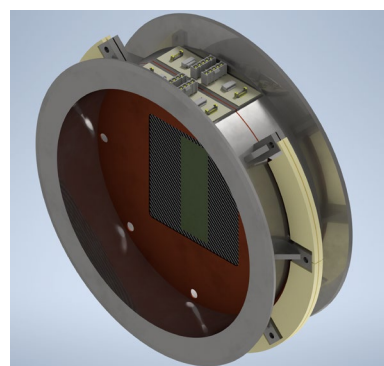
Measurement of low- Q^2 elastic-scattering

Detection of low-energetic recoil-protons and scattered muons with small scattering-angle.

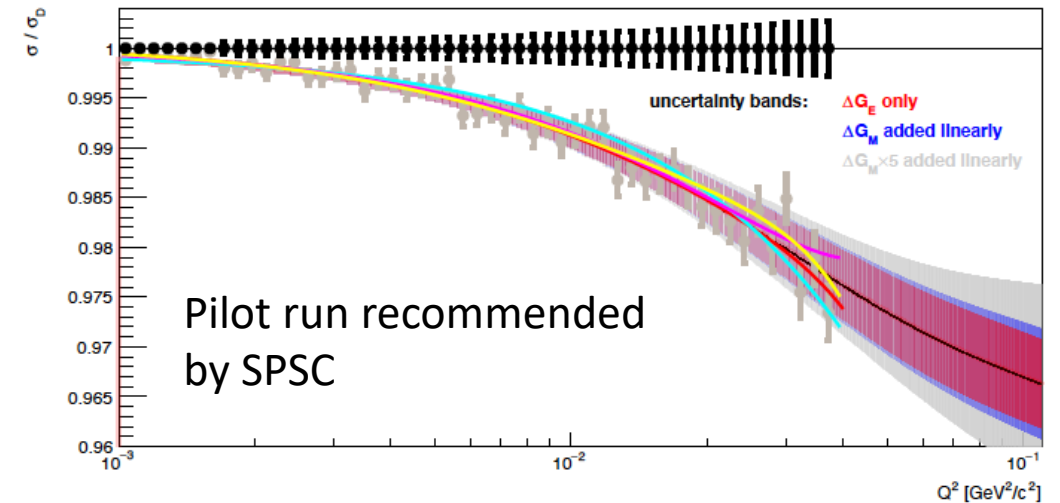
- Silicon trackers along large leaver-arm to measure small scattering-angles
- Fiber tracker timing and trigger (fallback)
- TPC as an active target with the ability to measure the low-energetic recoil-proton
- New continuously-running DAQ



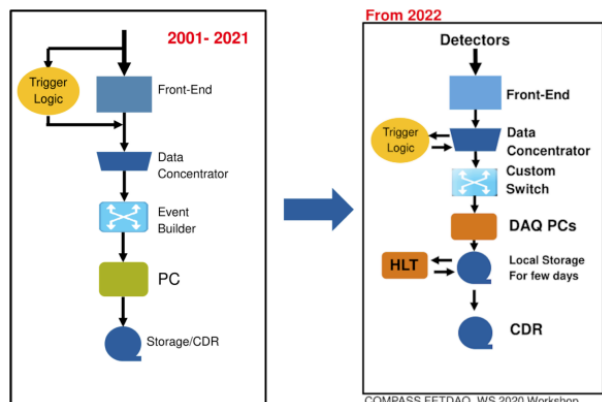
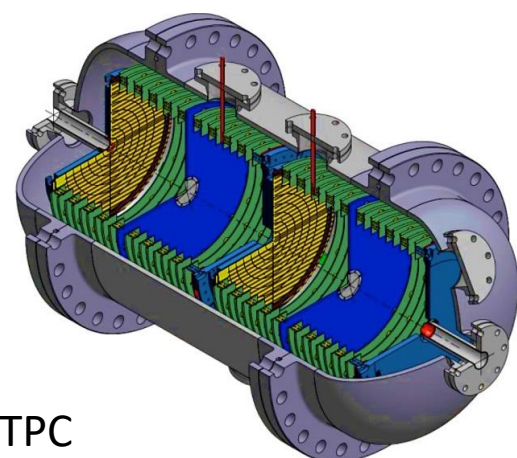
200 μ m fiber readout



20 bar H₂ TPC



- COMPASS spectrometer → Momentum measurement of scattered muon → Radiative background using electromagnetic calorimeter → Muon identification with muon filter and hodoscope



New TL DAQ

COMPASS has provided in the last 20 years a broad spectrum of results, still some questions like the emergency of the hadronic mass as well as the spin puzzle remain opened and of extreme interest.

In the tradition of the COMPASS spirit a wide spectrum of new measurements have been proposed by the COMPASS++/AMBER collaboration with conventional and RF separated beams

In 2021, 22 , 23 the COMPASS experiment will perform precise measurement on Transversity and the new collaboration will shed light on the proton radius puzzle.

Grazie